

RESEARCH ARTICLE

10.1002/2016WR019817

Little impact of the Three Gorges Dam on recent decadal lake decline across China's Yangtze Plain

Jida Wang¹ , Yongwei Sheng², and Yoshihide Wada^{3,4,5,6} 

¹Department of Geography, Kansas State University, Manhattan, Kansas, USA, ²Department of Geography, University of California, Los Angeles, Los Angeles, California, USA, ³International Institute for Applied Systems Analysis, Laxenburg, Austria, ⁴Center for Climate Systems Research, Columbia University, New York, New York, USA, ⁵NASA Goddard Institute for Space Studies, New York, New York, USA, ⁶Department of Physical Geography, Utrecht University, CS Utrecht, Netherlands

Key Points:

- The recent decadal lake decline in China's Yangtze Plain is a major result of climate variability, instead of direct human interventions
- The Three Gorges Dam (TGD) causes no major change in downstream climate given limited impacts on lake area and thus open water evaporation
- Impacts of human water consumption and Yangtze channel erosion are comparable to that of TGD flow regulation and may continue to grow

Supporting Information:

- Supporting Information S1

Correspondence to:

J. Wang,
jidawang@ksu.edu;
gdbruins@g.ucla.edu

Citation:

Wang, J., Y. Sheng, and Y. Wada (2017), Little impact of the Three Gorges Dam on recent decadal lake decline across China's Yangtze Plain, *Water Resour. Res.*, 53, 3854–3877, doi:10.1002/2016WR019817.

Received 20 SEP 2016

Accepted 1 APR 2017

Accepted article online 6 APR 2017

Published online 11 MAY 2017

Abstract The ubiquitous lakes across China's Yangtze Plain (YP) are indispensable freshwater resources sustaining ecosystems and socioeconomics for nearly half a billion people. Our recent survey revealed a widespread net decline in the total YP lake inundation area during 2000–2011 (a cumulative decrease of ~10%), yet its mechanism remained contentious. Here we uncover the impacts of climate variability and anthropogenic activities including (i) Yangtze flow and sediment alterations by the Three Gorges Dam (TGD) and (ii) human water consumption in agricultural, industrial, and domestic sectors throughout the downstream Yangtze Basin. Results suggest that climate variability is the dominant driver of this decadal lake decline, whereas studied human activities, despite varying seasonal impacts that peak in fall, contribute marginal fraction (~10–20% or less) to the interannual lake area decrease. Given that the TGD impacts on the total YP lake area and its seasonal variation are both under ~5%, we also dismiss the speculation that the TGD might be responsible for evident downstream climate change by altering lake surface extent and thus open water evaporation. Nevertheless, anthropogenic impacts exhibited a strengthening trend during the past decade. Although the TGD has reached its full-capacity water regulation, the negative impacts of human water consumption and TGD-induced net channel erosion, which are already comparable to that of TGD's flow regulation, may continue to grow as crucial anthropogenic factors to future YP lake conservation.

1. Introduction

China's Yangtze Plain (YP, Figure 1a), one of the World Wildlife Fund (WWF) terrestrial ecoregions, is an ~140k km² fluvial belt encompassing the middle and lower reaches of the Yangtze River, home to ~20% (12k km²) of the freshwater lake area in East Asia (inferred from the Shuttle Radar Topography Mission Water Body Dataset (SWBD)) [SWBD, 2005]. Distributed ubiquitously across the YP, these lakes are underpinning components of the biophysical environment [Du et al., 2011; Fang et al., 2005; Ma et al., 2014; Yang and Lu, 2013], providing the primary surface water storage to sustain local ecosystems, food security, and socioeconomic development for nearly half a billion people (inferred from the LandScan High Resolution Global Population Data) [Oak Ridge National Laboratory, 2008]. Influenced by the East Asian monsoon, most of these lakes exhibit great intraannual variation in inundation area, which interacts with the Yangtze River by nature [Wang et al., 2013]. However, intensive anthropogenic activities in the past decades, including the world's largest hydroelectric project, the Three Gorges Dam (TGD) [China Three Gorges Construction Yearbook Commission, 2004; Nilsson et al., 2005], may have significantly altered the natural hydrological regime of the Yangtze River and its relation with the alluvial environment, leading to severe vulnerabilities for today's YP lake system [Du et al., 2011; Fang et al., 2005; Feng et al., 2013; Qiu, 2011; Wang et al., 2014a, 2013].

Our recent survey [Wang et al., 2014a], using ~17k satellite images, further questions the resilience and future stability of this critical lake system by uncovering a widespread decline of the total lake inundation area across the YP from 2000 to 2011 (a cumulative decrease of 930 km² or 9.3%; Figure 1b). This decadal decline occurred concurrently with (i) serial meteorological droughts in the Yangtze hydrological basin [Feng et al., 2011a, 2013; Liu et al., 2013; Qiu, 2011; Wang et al., 2014a; Z. X. Zhang et al., 2015; Z. Z. Zhang et al., 2015], (ii) increasing water withdrawal and consumption driven by China's rapid economic expansion

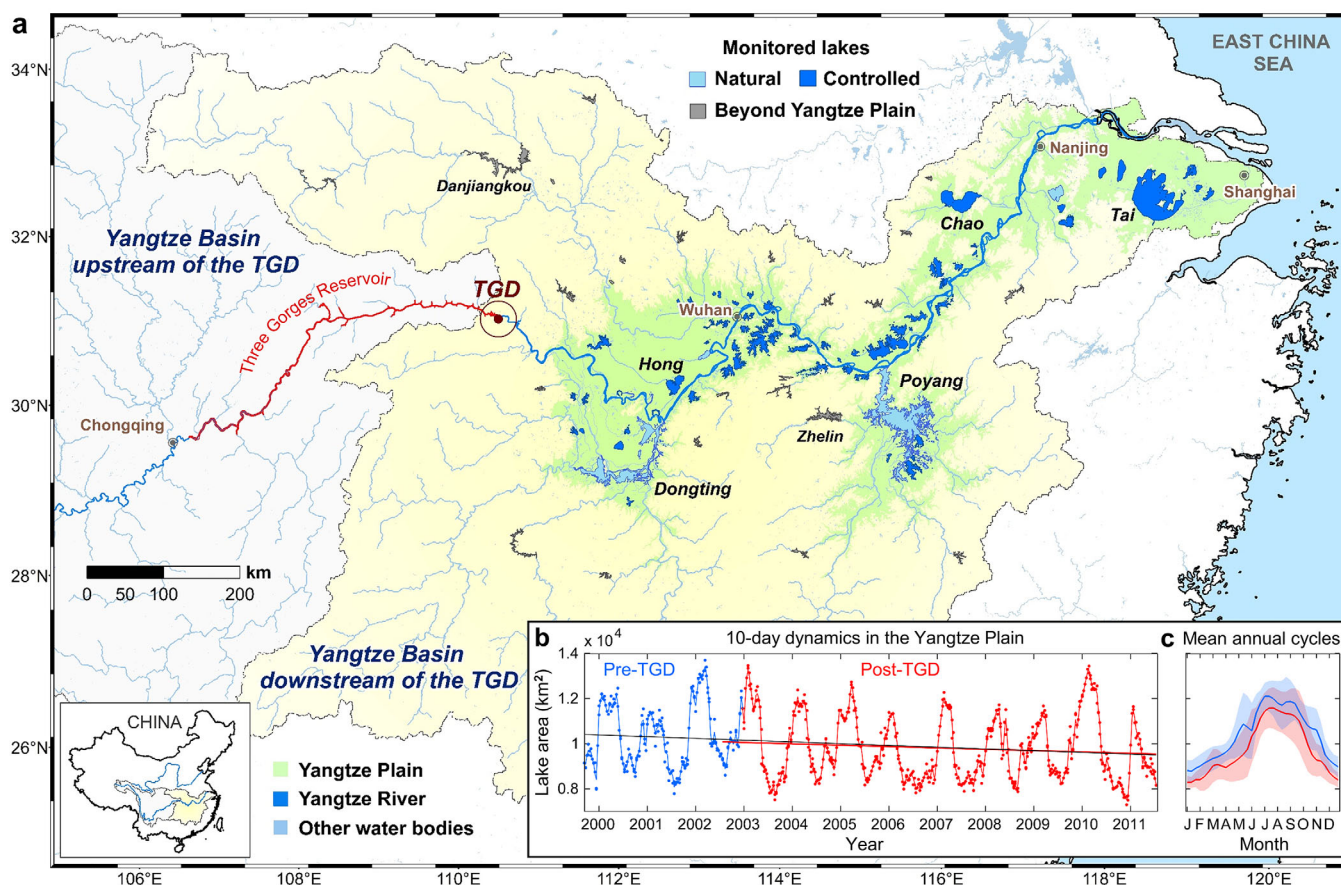


Figure 1. Monitored Yangtze hydrological basin and lake systems. (a) The Yangtze Basin downstream of the TGD (~784k km²). The monitored lake system across the YP (green) includes water bodies whose connections to the Yangtze River are natural (light blue) or controlled by floodgates (dark blue) [see Wang et al., 2014a for detailed statistics]. The outline of the Three Gorges Reservoir (TGR, red) is modified from the extent in the Global Reservoir and Dam Database, Version 1.1 (GRanDv1.1) [Lehner et al., 2011a, 2011b]. (b) Ten day dynamics of aggregated lake area in the YP, 2000–2011. Significant decreasing trends are revealed for both 2000–2011 (black) and the post-TGD period alone (i.e., after the initial TGD impoundment in June, 2003; red). Two common monotonic fitting methods, the best fit simple linear regression (SLR) and the nonparametric Kendall-Theil (KT) robust line [Theil, 1950], are used to compute all interannual trends throughout this paper. Values and significance levels produced by both methods are overall consistent. For simplicity, only SLR trends are reported in the main paper, while associated KT trends are given in supporting information. (c) Mean annual cycles of aggregated lake area in the YP during the pre-TGD and post-TGD periods (blue and red, respectively; lines represent means and shades standard deviations).

[Changjiang Water Resources Commission, 2000–2011; Wada et al., 2013; Yang et al., 2015], and (iii) the initial and yearly intensifying upstream water/flow regulation at the TGD [China Three Gorges Construction Yearbook Commission, 2011; Ou et al., 2012; Wang et al., 2013]. Despite a positive precipitation anomaly in 2010, the decreasing trend in lake area is significant in all seasons, with the most substantial decrease in fall (1.2–1.4% yr⁻¹) which coincides with the TGD water storage season. To effectively conserve this crucial freshwater storage, we need an immediate and thorough understanding of the explicit impact of each identified major factor, which hitherto remains largely unclear or contentious (see literature summary in supporting information Table S1).

Here we present a comprehensive investigation of the underlying mechanisms driving the decadal lake area decline across the YP. By integrating in situ measurements, remotely sensed observations, and a calibrated hydrological model, we quantify the influences of both climate variability and major anthropogenic activities including (i) Yangtze flow and sediment alterations by the TGD and (ii) human water consumption (i.e., net withdrawal) from the agricultural, industrial, and domestic sectors throughout the Yangtze Basin downstream of the TGD (hereafter “downstream Yangtze Basin”; Figure 1a). Our findings provide a timely advancement in assessing recent human interventions on the critical Yangtze hydrological system, and contribute additional scientific guidance to water resource managements in populated and rapidly developing regions during the global epoch of the Anthropocene [Crutzen, 2002].

2. Background

2.1. Lake System in the Yangtze Basin Downstream of the TGD

We conceptualize the contemporary lake system in the Yangtze Basin downstream of the TGD (a total lake area of $\sim 15\text{ k km}^2$) into three distinct groups (Figure 1a) [Wang *et al.*, 2014a]. Nearly 80% of the lakes in area are hosted by the YP (inferred from SWBD). These lakes are naturally influenced by the hydrological regime of the Yangtze River; however, after decades of artificial channel diversion, land reclamation, and floodgate management, only $\sim 20\%$ in area remain freely connected to the Yangtze River today, hereafter referred to as “natural lakes” (or Class I). Such lakes include China’s two largest freshwater lakes (i.e., Poyang and Dongting), Lake Shijiu, two oxbow lakes, and one flood storage zone. The other lakes on the YP have been artificially gated for flood-control, agricultural, or water-supply purposes, thus leading to partial to complete disconnection from the Yangtze River. They are hereafter referred to as “controlled lakes” (or Class II). The remaining 20% of the total lake area (Class III) is found in the form of man-made reservoirs in the tributaries upstream to the YP. Although unaffected by the Yangtze River, these reservoirs can regulate tributary flows which impact water supply to the downstream YP lakes.

2.2. Decadal Lake Area Changes

This study builds upon our previous finding of lake area dynamics in the downstream Yangtze Basin from February, 2000 to December, 2011 using MODIS Terra daily surface reflectance imagery (MOD09) [Wang *et al.*, 2014a, 2014b]. Studied lakes cover all water bodies larger than 20 km^2 across the downstream Yangtze Basin, including +85% of the total lake area within the YP (i.e., 100% and 81% of Class I and II lakes, respectively). These lakes were organized into 90 regions including 6 regions for Class I, 56 for Class II, and 28 for Class III (lake regions in Classes I and II shown in supporting information Figure S1). In each lake region, water extents were mapped from high-quality, cloud-free MODIS images with a targeted average mapping frequency of one snapshot per 10 days. Detailed lake mapping methods and quality assurance are provided in Wang *et al.* [2014a].

Our lake mapping revealed that nearly 70% of the total YP lake area (23 out of 62 Class I and II lake regions) underwent evident decline in this recent decade. By aggregating time series of inundation areas in all YP lake regions (Figure 1b), we calculated a significant net decreasing rate of $77.5\text{ km}^2\text{ yr}^{-1}$ ($0.8\%\text{ yr}^{-1}$) from 2000 to 2011 (a total decrease of 9.3%). To better contextualize TGD influences on the observed lake decline, we divided the complete monitoring period (2000–2011) into pre-TGD and post-TGD periods before and after the TGD’s initial water impoundment (i.e., June 2003). Consistent with the interannual trend in 2000–2011, a significant lake area decrease of $60.1\text{ km}^2\text{ yr}^{-1}$ (or $0.6\%\text{ yr}^{-1}$) persists in the post-TGD period. By comparing the mean annual cycles of lake area between the two periods, we identified an evident year-round drop of $641.8 (\pm 280.9)\text{ km}^2$ or $6.2 (\pm 2.7)\%$ after the TGD operation (Figure 1c), hereafter referred to as “the post-TGD lake decline.”

In contrast to lake decline within the YP, significant increasing trends were observed in nearly 70% of the total lake area (14 out of the 28 lake regions) beyond the YP during 2000–2011, leading to a net increasing rate of $9.2\text{ km}^2\text{ yr}^{-1}$ (a cumulative increase of 7.3%) in the aggregated inundation area of Class III reservoirs (change statistics for all individual lake regions provided in Wang *et al.* [2014a]). This contrast between lake and reservoir changes is also verified in terms of water storage across the entire Yangtze Basin from 2000 to 2014 by Cai *et al.* [2016].

3. Materials and Data Sets

Daily water regulations of the TGD (i.e., inflows and outflows) during 2000–2011 are acquired from the China Three Gorges Corporation [www.ctgpc.com.cn]. To quantify TGD’s impacts on the complete downstream reach, we collect hydrological measurements at 15 gauging stations along the Yangtze River immediately downstream from the TGD (st. 1) to Zhenjiang (st. 15) close to the estuary, including Chenglingji (st. 5) and Hukou (st. 10) at the outlets of Lakes Dongting and Poyang, respectively (see supporting information Figure S1 for station locations and IDs). Daily station levels and discharges during 2004–2011 are acquired from the Yangtze Waterway Bureau data available at www.cjhdj.com.cn. More descriptions of the gauging stations and discharge/level acquisition can be found in Wang *et al.* [2013].

Daily climate variables (e.g., precipitation and mean air temperature) are retrieved from the ERA-Interim reanalysis climate data archive [Dee et al., 2011] (European Center for Medium-Range Weather Forecasts data available at apps.ecmwf.int/datasets) to force the PCRaster Global Water Balance (PCR-GLOBWB) hydrological model for streamflow simulation. We refer to van Beek et al. [2011] and Wada et al. [2011a, 2011b, 2014b, 2016] for detailed model parameterization and routing scheme. To account for uncertainties in climate variables, we also obtain multiple precipitation and temperature data sets (refer to supporting information Figure S2) for the time series comparison between lake area and different climate variables.

Human water consumption is estimated considering the effects of not only population growth but also economic increase and changes in irrigated areas over the studied period at 0.1° spatial resolution [Wada et al., 2014b, 2016]. Historical daily water withdrawal and consumption for agricultural, industrial, and domestic sectors are estimated by using the latest available global data sets of socioeconomic (e.g., population and GDP), technological (e.g., energy and household consumption and electricity production), and agricultural (e.g., the number of livestock and irrigated areas) drivers [Wada et al., 2011a, 2011b]. A flow chart that describes how we compute sectoral water consumptions from various data sources is provided in supporting information Figure S3. The estimated sectoral water withdrawals (or gross water demand) have been calibrated against country statistics reported in the FAO AQUASTAT (Food and Agriculture Organization (FAO) data are available at www.fao.org/nr/water/aquastat/main) for China in order to obtain a more accurate intensity of annual water use over the study period 2000–2011.

4. Methods

We follow a schematic impact chain (Figure 2) to assess the contribution of each driving factor on the observed YP lake decline. This impact chain illustrates how the TGD, human water consumption, and climate variability affect critical hydrological variables (e.g., river flow, level, sediment transport, and channel cross-sectional geometry), and how the alterations propagate downstream to affect the YP lake system. Uncertainty analysis and limitations for each impact are provided in detail in supporting information.

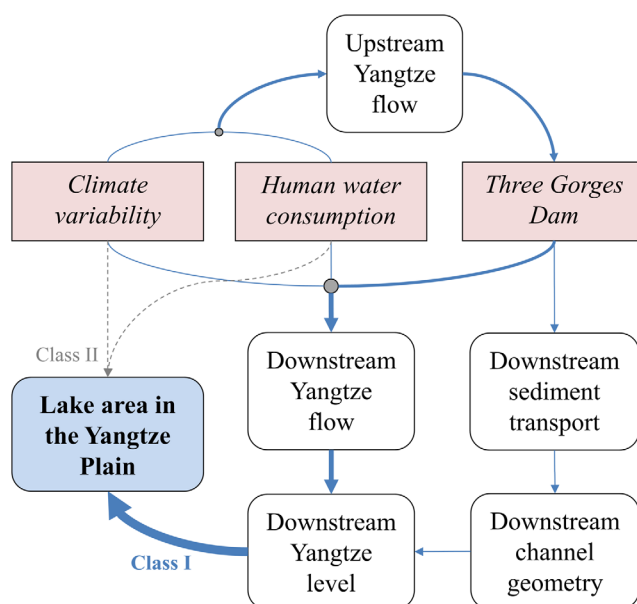


Figure 2. Schematic chain illustrating anthropogenic and climate factors and their downstream impacts on the YP hydrological regime. The thickness of each arrow connector reflects the number of factors that may accumulatively influence the next factor. Blue solid connectors represent impacts on the natural (Class I) lakes while grey dotted connectors represent impacts on the controlled (Class II) lakes.

4.1. Scenario Setup and Discharge Simulation

To facilitate method descriptions, we introduce five model scenarios which assume the exclusion of none to several anthropogenic factors from the downstream Yangtze Basin (Table 1). Each scenario defines a unique setting for surface flow, which then leads to differences in water level and lake area. Three separate runs with the PCR-GLOBWB model are performed to simulate daily discharges in the downstream Yangtze Basin during 2000–2011 under the *regulated*, *pristine*, and *realistic* scenarios, respectively. These runs are forced by the same climate condition but vary in anthropogenic inputs. In the first run (*regulated* scenario), the initial Yangtze flows (i.e., immediately downstream of the TGD) are calibrated by observed daily TGD outflows, in order to compute downstream discharges under TGD’s flow regulation (denoted as q_r). In the

Table 1. Model Scenarios With Different Inclusions of Anthropogenic and Climate Factors^a

Scenario	Definition				Flow	Level	Area
Observed	Remote Sensing or In Situ Measurements				Q	L	A
Modeled	Three Gorges Dam (TGD)		Human Water Consumption	Climate Variation			
	Flow Regulation	Channel Erosion					
<i>Realistic*</i>	✓	✓	✓	✓	q	l	a
<i>Regulated*</i>	✓	✓	×	✓	q_r	l_r	a_r
<i>Unregulated</i>	×	✓	✓	✓	q_u	l_u	a_u
<i>Consumed</i>	×	×	✓	✓	$q_c = q_u$	l_c	a_c
<i>Pristine*</i>	×	×	×	✓	q_n	l_n	a_n

^aDischarges under scenarios with "*" are directly simulated by the PCR-GLOBWB. "✓" and "×" indicate inclusion and exclusion of the associated factors, respectively.

second run (*pristine* scenario), the Yangtze flows are initiated by observed TGD inflows to simulate the natural downstream discharges driven by climate forcings alone (q_n). The use of TGD inflows assumes that recent human activities in the upstream Yangtze Basin do not alter the overall tendency of Yangtze discharges to the TGD, which is fairly corroborated by supporting information Figure S4 and recent efforts using both modeling and satellite remote sensing [e.g., Birkinshaw et al., 2016; Cai et al., 2016] (see more in section 5.3). In the third run (*realistic* scenario), observed TGD outflows are used to calibrate the initial Yangtze flows (as for *regulated* scenario), and estimated daily sectoral water consumptions (see section 3) are routed along the downstream drainage network together with climate variables. In other words, this run includes both climate variability and studied anthropogenic factors (i.e., TGD and human water consumption) to simulate more realistic discharges in the downstream Yangtze Basin (q). By comparing daily time series of q with station measurements, we identify time-lag errors of up to ~7–8 days in the simulated Yangtze flows, which are shorter than our focused 10 day time scale. These lag errors appear consistent among all three model runs and are removed from our simulations [see Wang et al., 2013 for details]. Lag-free simulations are next used to further derive discharges under the other two scenarios (*unregulated* and *consumed*), which are explained in the following sections. For clarity, we use lower case Roman letters to denote variables from modeled scenarios, upper case from observations (including gauging and satellite measurements), and Greek letters for relations/functions among variables. All symbol notations in this study are summarized in Appendix A.

4.2. Assessing Impacts of the TGD

Since its initial water impoundment in June 2003, the TGD has altered the downstream Yangtze regime in two primary ways: regulating the Yangtze water flow and reducing sediment load to the downstream Yangtze channel (Figure 2) [Wang et al., 2013]. According to the theory of stream channel hydraulic geometry [Leopold and Maddock, 1953], TGD-induced Yangtze flow changes trigger instant alterations of the Yangtze level (with an impact lag time of ~12 days to the estuary) [Wang et al., 2013], a critical variable of controlling water interactions between the Yangtze River and its freely connected fluvial lakes [Guo et al., 2012; Liu et al., 2013]. Previous studies [e.g., Liu et al., 2013; Wang et al., 2014a; Ye et al., 2014; Zhang et al., 2014] suggested that the inundation areas of Lakes Poyang and Dongting (both in Class I) are largely determined by their outlet/boundary conditions, here measured as Yangtze water levels at the confluence with the lake outflow. On the other hand, reduced sediment loads from the TGD lead to chronic erosion/incision along the downstream Yangtze channel [Dai and Liu, 2013; Xu and Milliman, 2009; Yang et al., 2006, 2007], which gradually changes the hydraulic geometry of river cross sections, including the stage-discharge (SD) rating. Changed Yangtze levels due to both flow regulation and channel erosion alter natural water gradients at lake outlets, thus enabling further changes in lake inundation pattern. Following such an impact chain, we adopt a three-step procedure to assess the influences of both TGD water regulation and induced net channel erosion on the YP lake area.

The first step identifies individual lakes that are constantly or at least conditionally impacted by the Yangtze River. This is done by examining the empirical relationship between daily inundation areas (A) and outlet water levels (L) for each lake region (in both Classes I and II). As described above, we consider a lake outlet to be the confluence of the Yangtze River and lake outflow, which may be slightly downstream from the lake pour point. Given any lake, if its outlet generally coincides with one of the 15 gauging stations (refer

back to section 3), levels measured at that gauging station are used directly to represent L ; otherwise, levels measured at a nearby gauging station are adjusted by the simulated discharge changes from that nearby station to the lake outlet, and used as a surrogate of lake outlet levels. For the latter situation, we have

$$L = \varphi_y \left(\varphi_y^{-1}(L^*) + q - q^* \right) \quad (1)$$

where φ_y denotes the in situ SD rating curve in a given year (y) at a nearby surrogate station (φ_y is calibrated yearly in order to reflect channel geometric changes through time), φ_y^{-1} the inverse yearly SD rating, L^* daily level measurements at the surrogate station, and q and q^* daily discharges at the lake outlet (i.e., lake-river confluence) and the surrogate station, respectively, simulated under the *realistic* scenario (Table 1). Importantly, L is not an estimate of the lake outlet level, but the level at the surrogate station if it had the same flow as the outlet (calibrated as $\varphi_y^{-1}(L^*) + q - q^*$). By doing so, we are able to associate the variation of surrogate station level with that of lake boundary condition without necessarily acquiring the exact outlet level. We ensure that the Yangtze River section between each lake outlet and its surrogate station to be as mass conserved as possible (i.e., no other substantial tributary confluence) in order to minimize the uncertainty caused by simulation errors. Names and locations of the gauging stations used for all YP lake regions are provided in supporting information Table S2. Yearly SD rating curves for these gauging stations can be found in Wang et al. [2013] and their fitting statistics in supporting information Table S3.

In the second step, daily outlet level changes induced by both flow regulation and net channel erosion during the post-TGD period are estimated using (i) yearly updated SD rating curves established from station measurements and (ii) hydrological model simulations calibrated by the TGD flows. We refer to Wang et al. [2013] for more detailed methods of calculating Yangtze level changes. In brief, two hypothetical scenarios are formulated to account for both TGD impacts on each lake outlet level (Table 1): an *unregulated* scenario assuming no flow regulation from the TGD but changing/actual cross-sectional geometry in the downstream Yangtze channel, and a *consumed* scenario assuming no flow regulation and no channel geometric changes since the TGD's closure (i.e., only under human water consumption). TGD-induced flow changes along the downstream Yangtze River (Δq_r) are estimated as $q_r - q_n$, which are further subtracted from in situ Q to derive discharges without TGD's water regulation (q_u). When gauging records are unavailable, e.g., during June–December, 2003, we attempt to calibrate q using rescaling relations between measurements and simulations available from 2004, and use it to substitute for Q . For each outlet, daily water levels under the *unregulated* scenario (l_u) are then estimated by q_u using yearly rating curves (we conservatively assume the rating curve for June–December, 2003 to be identical to that of 2004; see supporting information for uncertainty analysis), while levels under the *consumed* scenario (l_c) are estimated by q_u using the fixed rating curve in 2004 representing the benchmark channel geometry right after TGD's closure:

$$l_u = \varphi_y(q_u) \quad (2)$$

$$l_c = \varphi_0(q_u) \quad (3)$$

where φ_0 denotes the SD ratings in the benchmark year of 2004, and $q_c \equiv q_u$ as we consider flows to be invariant to channel changes.

In the third step, TGD-induced daily area changes in each lake region (i) are estimated by outlet level changes using the established A - L relations (η):

$$\Delta a_r = \begin{cases} \eta(L) - \eta(l_u), & i \in \text{I-01 to I-06, II-06, II-11, II-17, II-35} \\ 0, & i \in \text{others} \end{cases} \quad (4)$$

$$\Delta a_e = \begin{cases} \eta(l_u) - \eta(l_c), & i \in \text{I-01, I-02, I-04, I-05, II-11} \\ 0, & i \in \text{others} \end{cases} \quad (5)$$

where Δa_r and Δa_e denote lake area changes induced by flow regulation and net channel erosion, respectively. As further described in section 5.1, TGD-impacted area changes are considered for 10 out of 62 YP lake regions (supporting information Figure S1) where A and L show evident relations (see Figure 3 and supporting information Table S4). Δa_e is assessed on 5 lake regions (I-01, I-02, I-04, I-05, and II-11) which constitute 91.0% of the total area of the 10 TGD-impacted lake regions, whereas the remaining 5 much smaller

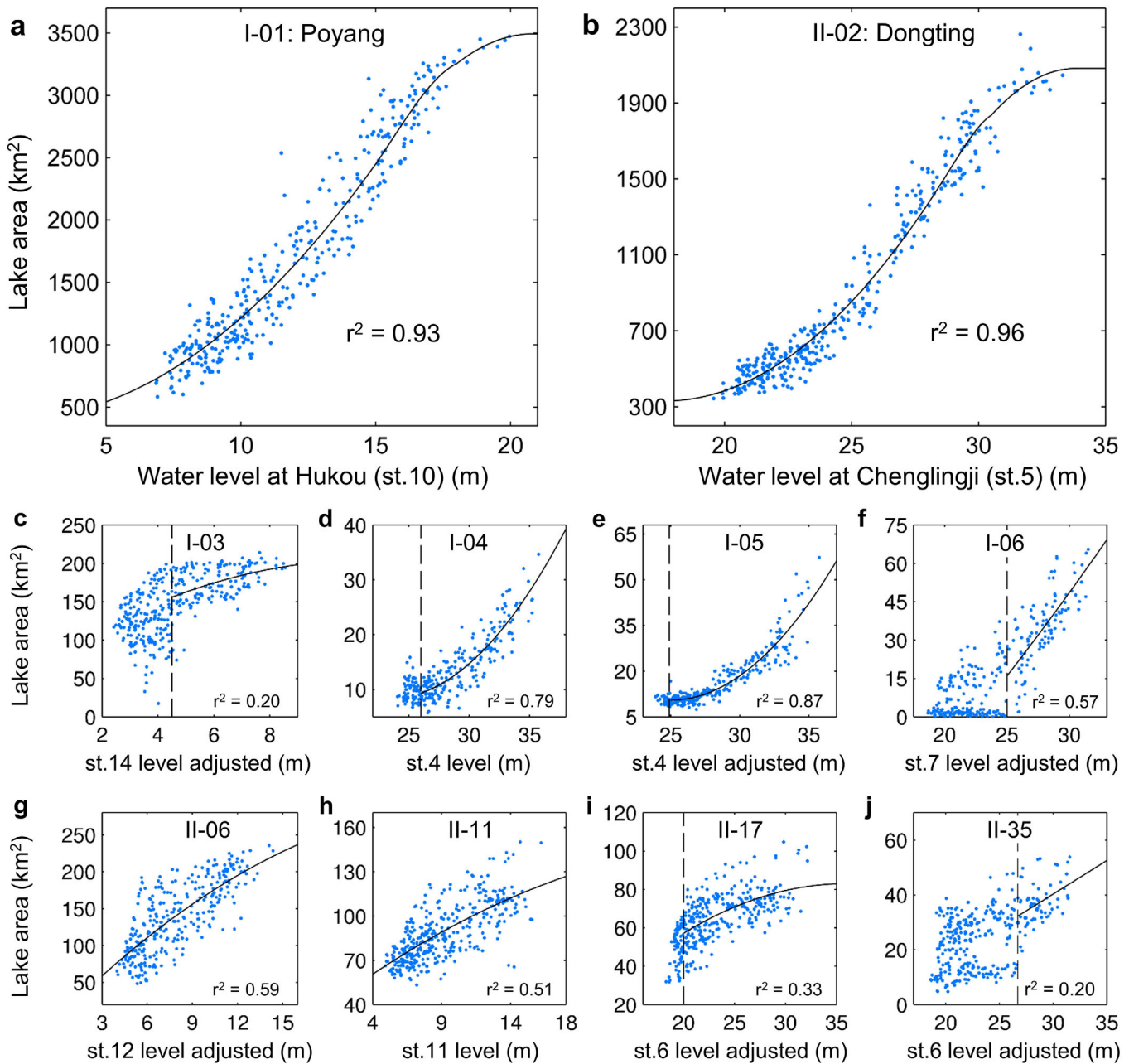


Figure 3. Relationships between mapped daily lake inundation areas and observed outlet Yangtze levels (2004–2011). Evident relations are identified in all Class I lakes, i.e., (a–f) I-01 (Poyang), I-02 (Dongting), I-03 (Shijiu), I-04 (Heiwa Ancient Channel, connected oxbow lake), I-05 (Yangtze Ancient Channel, connected oxbow lake), and I-06 (Dangwu, Nanwu, Daocao), and four Class II lakes, i.e., (g–j) II-06 (Caizi, Baitu, and Xizi), II-11 (Shengjin), II-17 (Huanggai), and II-35 (Chenhu). Refer to supporting information Figure S1 for locations of lake regions and gauging stations.

regions are excluded because their outlet levels are represented by nearby surrogate stations (see supporting information Table S2) where annual rating shifts may not reflect the precise channel geometric changes at the lake outlets. The total YP lake areas under no TGD influences (*consumed* scenario) are thus aggregated from the estimates of individual lake regions (a_c):

$$\sum_{i \in YP} (a_c)_i = \sum_{i \in YP} (A - \Delta a_r - \Delta a_e)_i \quad (6)$$

It is worth noting that cross-sectional changes in the downstream Yangtze River are dominantly but not completely attributed to the TGD. For example, *Yang et al.* [2014] estimated that the TGD explains over 70%

of the observed post-TGD (2003–2012) erosion along the Yangtze River between Yichang (st. 2) and Datong (st. 12), and nearly 90% of the reduced sediment discharge between 2001–2002 and 2003–2012 at Datong (st. 12). Therefore, even though our estimated Δa_e is assessed conservatively from the year 2004 and for 5 out of the 10 Yangtze-impacted lake regions, it may include contributions of (i) other human factors such as water impoundment in dams except the TGD, soil conservation, sand dredging, water diversion, and urbanization and (ii) climate-induced changes in surface runoff and thus sediment flow [Yang et al., 2015, 2014].

4.3. Assessing Impacts of Human Water Consumption

As the TGD alters water flow and sediment supply along the Yangtze River, only lakes freely connected to the main stem are under constant influence by the TGD. Human water consumption, nevertheless, occurs and accumulates along both the main stem and tributaries, thus producing a broader impact on the fluvial lake area across the YP. However, lacking sufficient documentation on local lake control, we restrict our assessment of the impacts of human water consumption on the inundation area of natural (Class I) lakes alone. Theoretically, this may result in a conservative estimate of the consumption-induced impacts across the YP but provides an original comparison of the relative influences between the TGD and water consumption on the critical natural lake system.

We progressively quantify the impacts of human water consumption on the Yangtze flow, lake outlet level, and lake inundation area, based on the same logic flow as used for assessing TGD impacts except that no change of channel cross-sectional geometry is considered as a consequence of human water consumption (Figure 2). Although water is consumed both upstream and downstream to the TGD, most consumption occurs in the densely populated downstream [Wada et al., 2014b]. Upstream consumption likely exerts a limited influence on the YP lake dynamics [Birkinshaw et al., 2016], given that upstream climate variation alone seems to already explain the observed interannual decrease in the TGD inflow (supporting information Figure S4). For this reason, we further emphasize the impact of human water consumption that is generated and then propagates in the downstream Yangtze Basin.

For each lake outlet, daily water levels assuming no human water consumption or the TGD (I_n under the *pristine* scenario) are estimated as

$$I_n = \varphi_0(q_c + \Delta q_c) \tag{7}$$

where Δq_c is calculated as q_r subtracting q , representing daily sectoral consumptions accumulated through the Yangtze main stem and tributary catchments up to the river-lake confluence. Daily impacts of human water consumption on inundation area (Δa_c) in each natural lake region are estimated as

$$\Delta a_c = \eta(I_c) - \eta(I_n) \tag{8}$$

The total inundation areas in the natural lake system (Class I) under no human impacts (*pristine* scenario) are thus aggregated from the estimates of individual lake regions (i):

$$\sum_{i \in I} (a_n)_i = \sum_{i \in I} (a_c - \Delta a_c)_i \tag{9}$$

To determine the contribution of human water consumption to the post-TGD decline (i.e., phase drop from pre-TGD to post-TGD mean annual cycles; refer back to Figure 1c), we further reconstruct the post-TGD lake inundation area under the condition of pre-TGD water consumption (a_c), in addition to the condition of no water consumption. Such results inform the contribution explicitly attributed to the net change of water consumption between the pre-TGD and post-TGD periods. For this purpose, we adopt the same approach as described above, except that Δq_c in equation (7) is replaced by $\Delta q_{\Delta c}$ representing daily consumption changes between the two periods:

$$\Delta q_{\Delta c} = (\Delta q_c)_{post} - \overline{(\Delta q_c)_{pre}} \tag{10}$$

where $(\Delta q_c)_{post}$ denotes daily water consumption in the post-TGD period and $\overline{(\Delta q_c)_{pre}}$ the mean daily water consumption in the pre-TGD period.

4.4. Assessing Impacts of Climate Variability

As we illustrate in Figure 2, Class I lake inundation area responds to outlet level which varies with lake-Yangtze confluence flow, whereas Class II inundation area is less influenced by the Yangtze River but more controlled by water supply from the tributary catchments. For either class, understanding natural river discharge across the downstream Yangtze Basin is a prerequisite for calculating lake area changes driven by climate variation.

Accordingly, we use simulated daily discharges under the *pristine* and *realistic* scenarios (Table 1) to assess the climate impact on the YP lake system. Different from the previous assessments, no gauging calibration is performed downstream of the TGD in order to exclude the impacts of nonstudied factors such as land cover land use changes (e.g., afforestation, soil conservation, and urbanization), water regulation in tributary reservoirs, and water diversion and transfer. Although these factors are not explicitly evaluated, the scale of their integrated impacts on the YP lakes may be implied by the fraction of lake area changes unexplained by our studied climate and human factors.

4.4.1. Natural (Class I) Lakes

Our previous assessments of human factors rely on in situ SD rating curves, which allows the inversion of human-induced flow changes to level changes with a precise adaptation of channel geometric shifts at each outlet station. However, the acquired station observations are limited to the post-TGD period, which is overall drier than the pre-TGD period, thus precluding a reliable rating extrapolation into high-flow conditions during the pre-TGD. Given this limitation, we use the *A-q* relations available during the entire study period of 2000–2011 to directly estimate climate-induced lake area changes, instead of using SD ratings and then *A-L* relations.

We assume that *q* under the *realistic* scenario, which combines both climate and anthropogenic impacts, can approach a sufficient explanation of the observed area variation in Class I lakes. Thus, for each lake region, daily lake areas (*a*) from 2000 to 2011 are estimated from the relationship (ψ) between mapped *A* and confluence *q* at the lake outlet; the estimation residuals are next adjusted by their seasonal relations (ξ) with lake catchment flow (*q'*):

$$a = \psi(q) + \xi(q') \tag{11}$$

The residual adjustment using catchment flow attempts to partially remedy the limitation of using simulated confluence flow as a substitute for outlet level: the latter is a result of complex lake-river hydrodynamics not fully captured in our routing scheme. Detailed equations for ψ and ξ are given in supporting information Table S5. Daily lake areas under the *pristine* scenario (*a_n*) are then estimated by inputting simulated natural discharges (*q_n*) to ψ and ξ .

Two solutions are next applied to evaluate the combined impact of climate variation and human activities. Solution 1 simply uses *a* estimated by *q*, while Solution 2 aggregates *a_n* and our previously quantified human impacts (i.e., Δa_r , Δa_e , and Δa_c) which involve in situ SD ratings and thus the impact of Yangtze channel changes.

4.4.2. Controlled (Class II) Lakes

The climate impact on each controlled lake region is assessed by the natural water supply from the lake catchment, simulated as daily *q_n* exiting the lake pour point (i.e., lake outflow). We use simulated outflow instead of inflow, in order to take into account evaporative loss above the lake region. To integrate the climate impact on the controlled lake system, we define a unitless index termed as *relative discharge* (*r_q*) by averaging standardized daily *q_n* from all lake regions based on the weight of mean lake size:

$$r_q = \left[\sum_{i \in II} \bar{A}_i \cdot (s_q)_i \right] / \sum_{i \in II} \bar{A}_i \tag{12}$$

where \bar{A}_i denotes the mean inundation area in any lake region *i* during 2000–2011 and *s_q* the standardized daily *q_n* from lake region *i*.

Lacking sufficient documentation about local lake water management, we are unable to explicitly partition Class II lake area changes into climate and anthropogenic contributions. Instead, our analysis seeks to understand whether the observed interannual lake changes are closely related to climate variation even with the existence of human seasonal management. For this purpose, we further explore Spearman's rank

correlations (ρ) between r_q and aggregated A on both 10 day and annual time scales. A significant positive correlation, if corroborated, suggests a likely important role of local climate in driving the decadal area decline in the controlled lake system. Such a method is also applied to understand the climate impact on the observed area increase in reservoirs beyond the YP (Class III lakes).

4.5. Uncertainty Analysis

We quantify the uncertainty from each of our above mentioned assessments, and integrate these multiple-source uncertainties to infer 95% confidence intervals for all major estimations (see section 5). The uncertainty sources include (i) yearly SD rating curves for estimating lake boundary levels (supporting information Table S3), (ii) lake A - L functions for estimating human-induced lake area changes (supporting information Table S4), and (iii) lake A - q functions for estimating climate-induced lake area changes (supporting information Table S5). Results from sources i and ii are combined to propagate the overall uncertainty of each estimated human impact (TGD flow regulation, net channel erosion, and human water consumption). The result of uncertainty source iii is used to further validate the fidelity of using simulated discharge to estimate lake inundation area and to compute the uncertainty of climate impact. Detailed uncertainty analysis is provided in supporting information, which also discusses lake mapping errors and the validations of simulated discharge and human water consumption. Our uncertainty analysis, however, does not include all possible error sources, such as simulation uncertainties when downstream gauging observations are absent (e.g., June–December 2003) and human-induced discharge changes upstream to the TGD.

5. Results

We reveal the quantified impact of each anthropogenic or climate factor as contributions to the change of lake area seasonality, the post-TGD lake decline (i.e., phase drop from pre-TGD to post-TGD mean annual cycles), and the interannual decreasing trends after 2000 and the TGD's initial operation.

5.1. How Much Does TGD Contribute to the Yangtze Lake Decline?

As shown in Figure 3, evident correlations between inundation area (A) and outlet level (L) exist in all six natural (Class I) lake regions. These relations can be generalized by single or compound quadratic functions (with most r^2 values close to or greater than 0.80), depicting changing sensitivity of ΔA to ΔL from low-flow to high-flow seasons (see supporting information Table S4 for fitting equations and statistics). No significant relations are found in the majority of controlled (Class II) lakes except four regions (II-06, II-11, II-17, and II-35), confirming a constant water management for most controlled lakes. Given such evidence, we consider that direct TGD impacts are limited to natural lakes and the four identified controlled lake regions. In general, the sensitivity of ΔA to ΔL tends to be weakened as L lowers. For several small regions (i.e., I-03 to I-06, II-17, and II-35), A appears to have little or no relation with L below certain thresholds (left of the dashed lines in Figures 3c–3f, 3i, and 3j), which may be partially due to our mapping uncertainties using MODIS imagery (see supporting information for uncertainty analysis). For each of these regions, when L falls below the identified threshold, we assume that the concurrent lake water surface is disconnected from the Yangtze River and thus not directly influenced by the TGD.

Figure 4 presents, to our best knowledge, the first reconstruction of the post-TGD mean annual cycle of aggregated lake area across the YP assuming no TGD influence. This result indicates an altered intraannual pattern in lake inundation area, primarily manifested by the changes under TGD's seasonal water dispatches [China Three Gorges Construction Yearbook Commission, 2004; Ou et al., 2012; Wang et al., 2013]. In such an annual cycle, the Three Gorges Reservoir (TGR) starts to reduce Yangtze flow and elevates the reservoir level around mid-September–October (namely the water-storage dispatch) in order to prepare for power generation. As a result, water levels along the entire downstream Yangtze River decrease by an average of ~ 0.2 – 1.0 m (a longitudinal range between Yichang and Zhenjiang gauging stations; see supporting information Figure S1 for station locations). These TGD-induced Yangtze level reductions temporally coincide with the natural flow recession, and thus accelerate water drainage from the connected lake system, causing an average decrease in total lake inundation area to be 235.7 km^2 or 2.2% (Figures 4a and 4b). This decrease is equivalent to 19.9% of the intraannual lake area variation across the YP, and explains 33.4% of the post-TGD lake decline observed in this storage season.

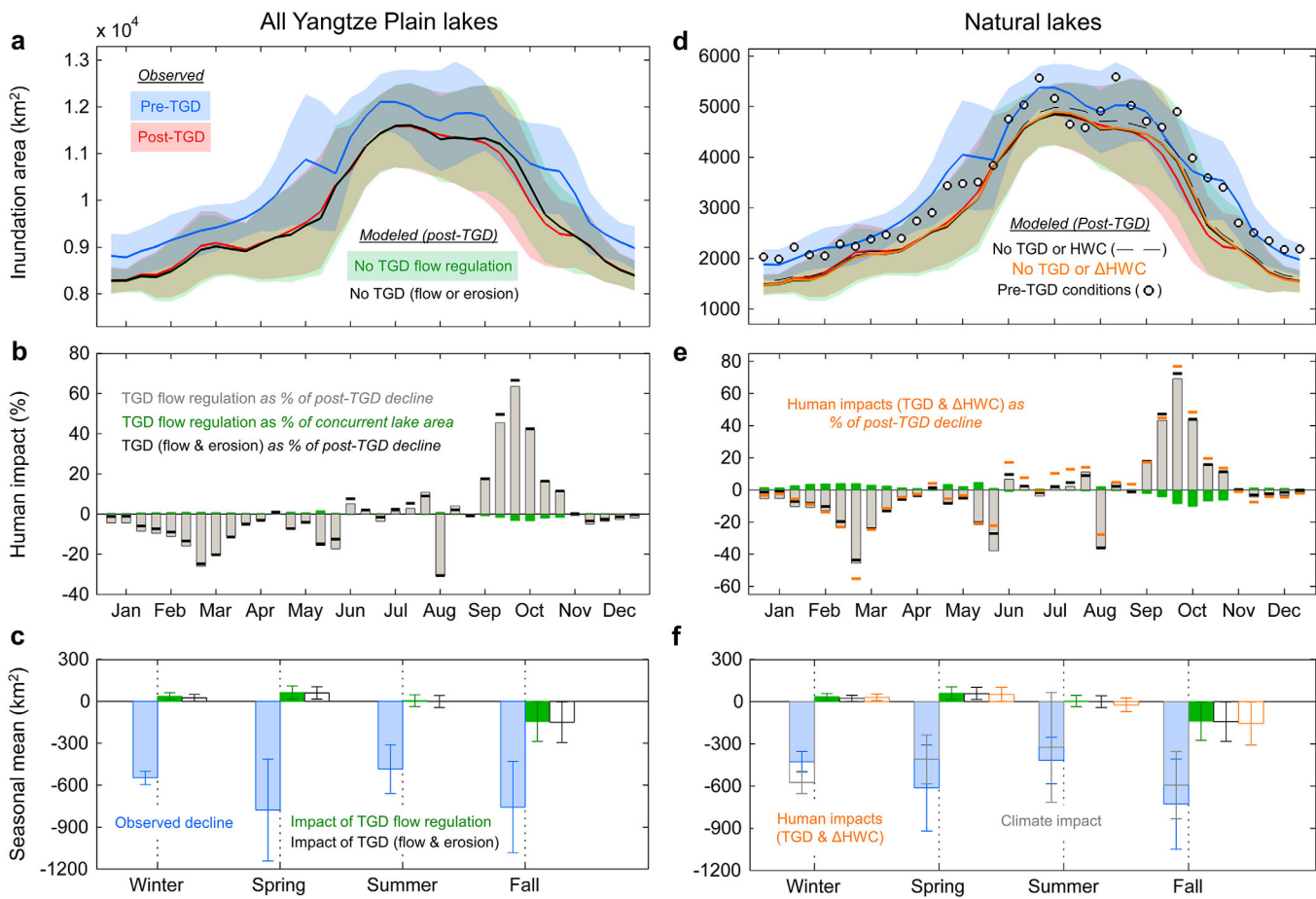


Figure 4. Anthropogenic and climate impacts on intraannual lake area variation during the post-TGD period (June 2003 to December 2011). Illustration of the impacts on aggregated inundation area in (a–c) all YP lakes and (d–f) natural lakes alone. Assessed impacts are compared on the context of the observed post-TGD lake decline. (a, d) Ten day mean annual cycles of observed and modeled lake areas (shaded areas illustrate lake area standard deviations). “HWC” represent human water consumption and “ Δ HWC” the change of HWC from pre-TGD to post-TGD periods. Green, black, and orange lines (illustrating “No TGD flow regulation,” “No TGD (flow or erosion),” and “No TGD or Δ HWC”) are closely above each other. Dots illustrate modeled post-TGD lake areas assuming pre-TGD conditions, i.e., (i) no TGD and (ii) water consumption and climate both the same as those in the pre-TGD period. (b, e) Ten day mean annual cycles of relative human impacts (“concurrent lake areas” in Figure 4b refers to estimated lake areas assuming no TGD’s flow regulation). (c, f) Mean seasonal contributions to the observed post-TGD lake decline (error bars illustrate standard deviations of assessed impacts within each season).

The TGR water level is steadily lowered under the following water-supplement dispatch in January–March. Opposite the previous water storage season, increased outflow from the TGD elevates the downstream Yangtze level by ~ 0.1 – 0.6 m, which slightly increases the YP lake area by 55.0 km^2 or 0.6% , accounting for 4.6% of its intraannual/seasonal variation. This area increase counteracts 11.4% of the concurrent post-TGD lake decline, and thus alleviates water scarcity during the winter monsoonal dry season. The TGD further releases water under the predischarge dispatch in May–early June to increase TGR’s summer flood storage. This continuous flow release increases the downstream Yangtze level by ~ 0.1 – 0.7 m, which reinforces its natural level rise during the spring rainy season. The TGD-induced Yangtze level rise tends to constrain outflows from the connected lakes to the Yangtze River and thus increases lake area by 87.6 km^2 or 0.9% . This influence is equivalent to 7.4% of the intraannual lake area variation, and similar to the winter water-supplement dispatch, counteracts the post-TGD lake decline by 9.3% . Finally, during the flood-control dispatch in July–August, the TGD stabilizes the Yangtze outflow and mitigates flood pressure by reducing the natural level variation along the downstream Yangtze River by ~ 14.0 – 36.0% . Consequently, the lake area variation in the flood season was reduced by 18.1% , despite a negligible impact on the concurrent lake area mean (7.3 km^2 or $<0.1\%$).

Meanwhile, reduced sediment loads released from the TGD lead to slow but enduring channel incision along a large portion of the downstream Yangtze River [Dai and Liu, 2013; Wang et al., 2013; Yang et al., 2006]. Over time, the lowered Yangtze level complicates the seasonal impacts on lake inundation induced

Table 2. Estimates of Anthropogenic and Climate Contributions to Post-TGD Lake Decline^a

Post-TGD Lake Decline	Seasonal Means (km ²)				Annual Mean (km ²)
	Winter	Spring	Summer	Fall	
All Yangtze Plain Lakes					
Observed	-547.1	-777.8	-484.7	-756.5	-641.5
Anthropogenic Impacts (Cumulative)					
TGD flow regulation	37.3 (±517.4) -6.8 (±94.6)% <i>p.</i> 0.027	62.8 (±420.3) -8.1 (±54.0)% <i>p.</i> < 0.001	4.2 (±454.9) -0.9 (±93.8)% <i>p.</i> 0.035	-144.6 (±538.8) 19.1 (±71.2)% <i>p.</i> 0.026	-10.1 (±486.0) 1.6 (±75.8)% <i>p.</i> 0.011
Channel erosion	25.4 (±519.4) -4.7 (±94.9)% <i>p.</i> 0.031	59.9 (±424.9) -7.7 (±54.6)% <i>p.</i> < 0.001	-0.7 (±462.1) 0.1 (±95.3)% <i>p.</i> 0.040	-149.7 (±543.0) 19.8 (±71.8)% <i>p.</i> 0.029	-16.3 (±490.4) 2.5 (±76.5)% <i>p.</i> 0.013
Natural (Class I) Lakes					
Observed	-428.4	-613.3	-417.8	-728.1	-546.9
Anthropogenic Impacts (Cumulative)					
TGD flow regulation	34.8 (±511.7) -8.1 (±119.5)% <i>p.</i> 0.076	59.4 (±415.3) -9.7 (±67.7)% <i>p.</i> 0.002	4.1 (±450.6) -1.0 (±107.9)% <i>p.</i> 0.067	-138.4 (±534.2) 19.0 (±73.4)% <i>p.</i> 0.031	-10.0 (±481.1) 1.8 (±88.0)% <i>p.</i> 0.029
Channel erosion	23.3 (±513.6) -5.4 (±119.9)% <i>p.</i> 0.085	56.9 (±419.9) -9.3 (±68.5)% <i>p.</i> 0.002	-0.4 (±457.9) 0.1 (±109.6)% <i>p.</i> 0.074	-143.1 (±538.6) 19.7 (±74.0)% <i>p.</i> 0.033	-15.8 (±485.6) 2.9 (±88.8)% <i>p.</i> 0.032
Water consumption	30.7 (±514.9) -7.2 (±120.2)% <i>p.</i> 0.081	50.2 (±420.1) -8.2 (±68.5)% <i>p.</i> 0.002	-23.4 (±455.8) 5.6 (±109.1)% <i>p.</i> 0.090	-155.2 (±538.9) 21.3 (±74.0)% <i>p.</i> 0.037	-24.4 (±485.6) 4.5 (±88.8)% <i>p.</i> 0.035
Climate impact	-574.2 (±742.3) 134.1 (±173.3)% <i>p.</i> 0.700	-410.0 (±1222.4) 66.9 (±199.3)% <i>p.</i> 0.744	-324.6 (±1340.3) 77.7 (±320.8)% <i>p.</i> 0.892	-594.9 (±1575.0) 81.7 (±216.3)% <i>p.</i> 0.868	-475.9 (±1262.0) 87.0 (±230.8)% <i>p.</i> 0.912
Both Impacts Combined					
Solution 1	-511.1 (±742.3) 119.3 (±173.3)% <i>p.</i> 0.877	-341.8 (±1222.4) 55.7 (±199.3)% <i>p.</i> 0.758	-356.4 (±1340.3) 85.3 (±320.8)% <i>p.</i> 0.949	-785.8 (±1575.0) 107.9 (±216.3)% <i>p.</i> 0.960	-498.8 (±1262.0) 91.2 (±230.8)% <i>p.</i> 0.958
Solution 2	-543.5 (±903.4) 126.9 (±210.9)% <i>p.</i> 0.860	-359.8 (±1292.6) 58.7 (±210.8)% <i>p.</i> 0.786	-347.9 (±1415.7) 83.3 (±338.8)% <i>p.</i> 0.945	-750.1 (±1664.6) 103.0 (±228.6)% <i>p.</i> 0.985	-500.3 (±1352.2) 91.5 (±247.3)% <i>p.</i> 0.962

^aContributions to seasonal and annual means of lake area decline are provided for (i) studied anthropogenic factors alone, where the impacts of TGD's flow regulation, net channel erosion, and change of human water consumption (between pre- and post-TGD periods) cumulatively add up, (ii) climate variation alone, and (iii) anthropogenic and climate factors combined. All contributions are quantified in terms of mean magnitude, uncertainty, and significance, which are reported in each cell as (i) area change in km² followed by its 95% confidence interval (CI) in parentheses (the upper row), (ii) area change as percentage of post-TGD decline (the middle row), and (iii) probability of the observed decline as a result of this contribution (the lower row), calculated as the *p* value of a one-sample *z* test that examines the difference of the observed decline from our estimated mean with its uncertainty. Two alternative solutions (see section 4.4.1) are used to summarize anthropogenic and climate contributions with highly consistent results.

by flow regulation. With reference to the initial channel condition in 2003–2004, the net downstream erosion during our studied post-TGD period counteracts the Yangtze level increases expected in winter and spring by an average of ~48% (varying from -25.1% to 138.8% among different stations) and ~35% (-13.3% to 80.4%), respectively. The expected level decrease in fall is, on the contrary, further reinforced by ~13% (-12.5% to 57.4%). Such erosion-induced impacts appear less evident on lake area (Figures 4a and 4b), with average counteraction of 31.7% in winter and 4.7% in spring, and reinforcement of 3.5% in fall (Figure 4c). Combining both impacts of flow regulation and net channel erosion, the TGD slightly reduces the total YP lake area by an annual mean of 1.7% (maximally 3.5%) and the intraannual lake area variation by 2.8% (Figure 4b).

We further summarize TGD's contributions to seasonal lake declines in Table 2 by including 95% uncertainty intervals and probabilistic confidence that the observed lake declines are attributed to the TGD alone (see supporting information for detailed uncertainty analysis). The integrated impact of the TGD contributes 149.7 km² or 19.8% to the post-TGD lake decline in fall but yields no evident explanation of the observed decline in the other seasons, or only accounts for a marginal 2.5% of the average annual decline. This is also corroborated by all seasonal *p* values of 4% or less, indicating low statistical probabilities that our assessed TGD impacts, despite inevitable uncertainties, could result in the observed YP lake decline.

As an important note, TGD's seasonal water regulation was gradually intensified from the initial impoundment until the full-operation capacity was first achieved in 2010 [see Wang *et al.*, 2013 for TGD hydrograph];

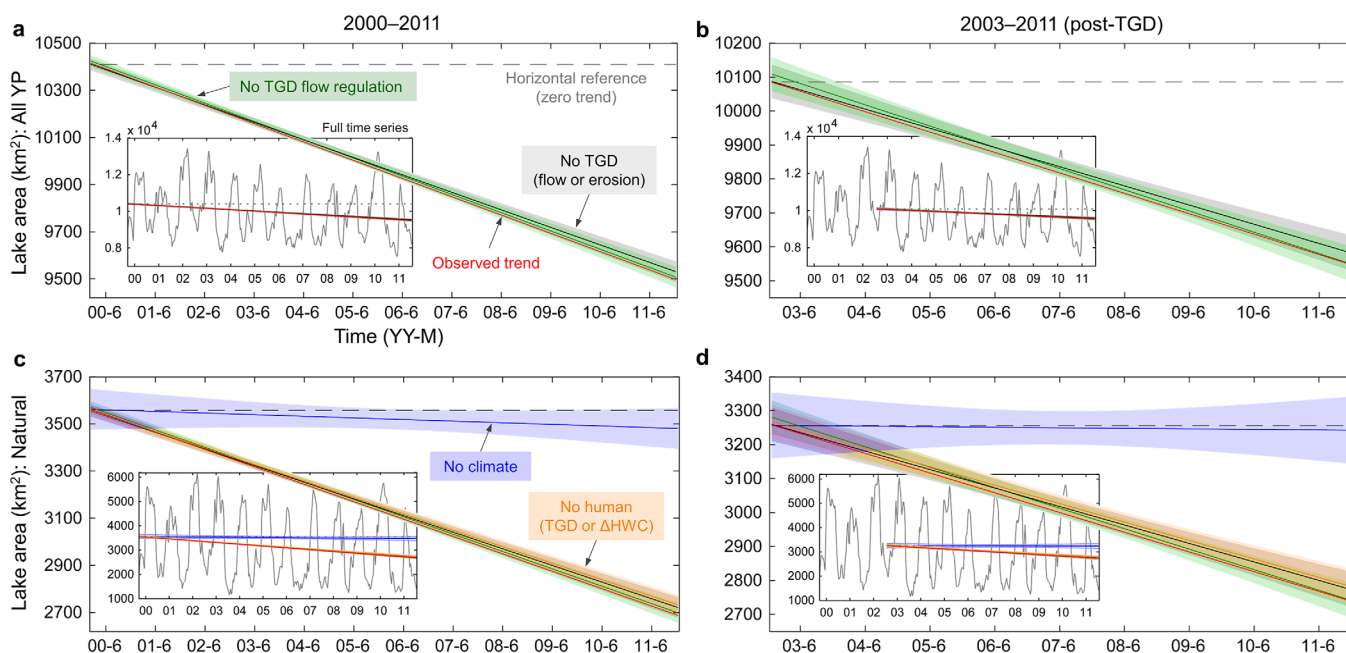


Figure 5. Anthropogenic and climate impacts on interannual lake area dynamics during 2000–2011. The contribution of each studied factor to the observed lake area decreasing trend during (left) (a, c) 2000–2011 or (right) (b, d) 2003–2011 (post-TGD) is quantified as a monotonic SLR line fitted on the modeled 10 day lake area series assuming no such impact, in all (top) (a, b) YP lakes or (bottom) (c, d) natural lakes alone. “No climate” illustrates the trend in lake area assuming no climate variation, calculated from the time series of observed lake areas (A) subtracting modeled realistic lake areas (a). Each shaded area illustrates a 95% CI for the generated linear trend arising from our estimation uncertainties (refer to supporting information for detailed uncertainty analyses). Figure insets show the full extent of observed 10 day lake dynamics overlaid by estimated monotonic trends and CIs.

therefore, our discussed seasonal impacts thus far represent the average effect of the TGD operation during the studied post-TGD period. The yearly amplified lake area reduction induced by TGR’s water-storage dispatch accelerated significantly the post-TGD decreasing trend in fall by $33.8 \text{ km}^2 \text{ yr}^{-1}$ or 42.5%, accounting for 29.8% of the observed decreasing trend in fall (supporting information Figure S5 and supporting information Table S6). Nevertheless, as TGR’s initial impoundment reduced the downstream lake area in June, 2003 and the following cyclic water release increased the downstream lake area in both spring and winter, TGD’s flow regulation turns out to have little negative contribution to the overall interannual lake area trend across the YP (Figures 5a and 5b and Table 3). Regardless of the seasonal variation in flow regulation, the Yangtze channel has constantly deepened since the closure of the TGD due to scouring, and together with flow regulation, contributes $4.2 (\pm 6.6)\%$ of the observed decreasing trend in the YP lake system during 2000–2011 and $5.9 (\pm 16.3)\%$ during the post-TGD period. Similarly, we take into account our estimation uncertainties to calculate negligible probabilities ($<0.1\%$) of the causality between the TGD and observed interannual lake decreasing trends (Table 3). Echoing our previous findings, these results suggest that the TGD operation has evident seasonal impacts on the downstream lake inundation, but is not a dominant factor to the recent lake decline across the YP.

5.2. How Does the TGD Compare to Human Water Consumption?

In the densely populated Yangtze Basin, about 40–50% of human water withdrawal is consumed without being returned to the river network [Changjiang Water Resources Commission, 2000–2011; Wada et al., 2014b, 2013]. Such water consumption (60–70% via agricultural irrigation) leads to local flow reductions which propagate downstream to substantive totals likely comparable to TGD’s regulation. Despite a slightly decreasing irrigation demand in the recent decade, the total water consumption remained to rise in the Yangtze Basin due to expanding industrial and domestic sectors [Changjiang Water Resources Commission, 2000–2011; Yang et al., 2015]. Thus, assessing the impact of human water consumption appears critical to developing a thorough understanding of the decadal YP lake decline. As stated in section 4.3, we focus on natural (Class I) lakes due to a lack of water management data for the controlled (Class II) lakes.

During our studied post-TGD period, human water consumption from the agricultural, industrial, and domestic sectors reduced the average annual flow along the downstream Yangtze River by $\sim 0.3\text{--}6.0\%$,

Table 3. Estimates of Anthropogenic and Climate Contributions to Lake Decreasing Trends^a

Interannual Lake Decreasing Trend	2000–2011		2003–2011 (Post-TGD)	
	Rate (km ² yr ⁻¹ , % yr ⁻¹)	Contribution	Rate (km ² yr ⁻¹ , % yr ⁻¹)	Contribution
All Yangtze Plain Lakes				
Observed	-77.5, -0.8 <i>p</i> < 0.001		-60.1, -0.6 <i>p</i> 0.022	
Anthropogenic Impacts (Cumulative)				
No TGD flow regulation	-77.4 (±5.1), -0.8 (±0.1) <i>p</i> < 0.001	0.1 (±6.5)% <i>p</i> < 0.001	-62.6 (±9.8), -0.6 (±0.1) <i>p</i> 0.026	-4.1 (±16.3)% <i>p</i> < 0.001
No channel erosion	-74.3 (±5.1), -0.7 (±0.1) <i>p</i> < 0.001	4.2 (±6.6)% <i>p</i> < 0.001	-56.5 (±9.8), -0.6 (±0.1) <i>p</i> 0.040	5.9 (±16.3)% <i>p</i> < 0.001
Natural (Class I) Lakes				
Observed	-73.8, -2.4 <i>p</i> < 0.001		-58.1, -1.9 <i>p</i> 0.023	
Anthropogenic Impacts (Cumulative)				
No TGD flow regulation	-73.6 (±5.0), -2.4 (±0.2) <i>p</i> < 0.001	0.3 (±6.8)% <i>p</i> < 0.001	-60.3 (±9.7), -2.0 (±0.3) <i>p</i> 0.014	-3.9 (±16.7)% <i>p</i> < 0.001
No channel erosion	-70.5 (±5.0), -2.3 (±0.2) <i>p</i> < 0.001	4.4 (±6.8)% <i>p</i> < 0.001	-54.4 (±9.7), -1.8 (±0.3) <i>p</i> 0.023	6.3 (±16.8)% <i>p</i> < 0.001
No water consumption	-69.7 (±5.1), -2.2 (±0.2) <i>p</i> < 0.001	5.5 (±6.9)% <i>p</i> < 0.001	-54.3 (±9.8), -1.8 (±0.3) <i>p</i> 0.024	6.5 (±16.8)% <i>p</i> < 0.001
Climate Impact				
No climate variability	-6.9 (±12.7), -0.2 (±0.4) <i>p</i> 0.149	90.7 (±17.2)% <i>p</i> 0.298	-1.6 (±19.0), -0.1 (±0.6) <i>p</i> 0.397	97.3 (±32.7)% <i>p</i> 0.871
Both Impacts Combined				
Solution 1	-3.2 (±12.7), -0.1 (±0.4) <i>p</i> 0.310	95.7 (±17.2)% <i>p</i> 0.621	-1.5 (±19.0), -0.1 (±0.6) <i>p</i> 0.427	97.4 (±32.7)% <i>p</i> 0.878
Solution 2	-2.8 (±13.6), -0.1 (±0.4) <i>p</i> 0.331	96.3 (±18.5)% <i>p</i> 0.690	2.2 (±21.3), 0.1 (±0.7) <i>p</i> 0.270	103.7 (±36.7)% <i>p</i> 0.841

^aEach cell in columns “rate” shows both absolute and relative interannual rates (in km² yr⁻¹ and % yr⁻¹, respectively), with 95% CIs (in parentheses), of the observed or estimated 10 day lake area series with cumulative removal of each factor, calculated by both SLR (reported in this table) and KT robust line (supporting information Table S7), followed by *p* value quantifying the significance of fitted decreasing trends (i.e., probability that the estimated rate equals zero). “Contribution” shows the change of interannual rate by each factor as percentage of the observed lake decreasing rate, followed by the probability of the observed decreasing rate as a result of this contribution, calculated as the *p* value of a one-sample *z* test that examines the difference of the observed lake decreasing rate from our estimated rate with its uncertainty. Here, “no channel erosion” and “no water consumption” indicate that Yangtze channel cross-sectional geometries and downstream human water consumption during the post-TGD period remain at the pre-TGD levels (i.e., the year 2004 for channel geometry and the average of ~2000-2003 for water consumption), respectively. Two solutions are used to integrate both anthropogenic and climate contributions as described in section 4.4.1.

leading to a level decrease of ~0.1–3.0%. Such level decrease is significant enough to reduce the total natural lake area by 77.2 km² or 2.6% (Figure 4d). Unlike the TGD’s influence, the impact of human water consumption stays negative in all seasons, which equals 81.5% of the TGD-induced lake area decrease in fall and completely counteracts the TGD-induced lake area increase by nearly 3 times in winter. Averaged annually, the consumption-induced lake area reduction exceeds the TGD impact by 61.3 km² or nearly 5 times.

However, the regional human water consumption increased at a slow rate during the study period (~1–3% yr⁻¹; supporting information Figure S6). The consequential lake area decrease, therefore, adds only marginal contributions to both the post-TGD decline (Figures 4d–4f and Table 2) and the interannual trends (Figures 5c and 5d and Table 3). On the studied natural lake system, anthropogenic impacts (combining both the TGD and human water consumption) account for 21.3%, 5.6%, and 4.5% of the post-TGD decline in fall, summer, and annual average, respectively (Figure 4f), and explain 5.5 (±6.9)% and 6.5 (±16.8)% of the decreasing trends for 2000–2011 and the post-TGD period, respectively (Figures 5c and 5d). Incorporating our estimation uncertainties (Tables 2 and 3), we shows an upper bound probability of only ~9% (mostly under 5%) that the combined human impacts equal the observed lake area changes. The dominant factor that has driven the primary lake decline across the YP, therefore, appears to be exogenous to these studied human activities.

5.3. Is Climate a Dominant Factor to the Yangtze Lake Decline?

Climate variations in precipitation, temperature, and evapotranspiration contribute to natural changes in fluvial lake inundation by driving local meteorology and altering surface runoff. Since entering the current millennium, the Yangtze Basin has been plagued by a series of extreme climate events, e.g., the summer

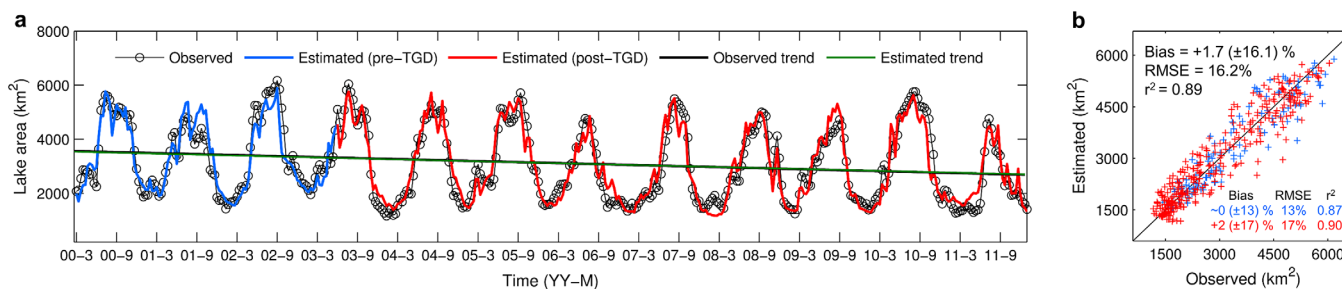


Figure 6. Validation of estimated Class I lake inundation areas with MODIS observations. (a) Ten day time series with SLR trends. (b) Cross-validation. Errors in the estimated lake areas (a in equation (11)) reflect uncertainties that may be propagated from climate data, human water consumption, discharge simulation, lake mapping, and area-discharge fitting. Estimates align generally well with MODIS observations, with +95% of the observed interannual decreasing trend replicated by the estimates (Figure 6a), ~2% mean bias, 13–17% RMSE, and ~0.90 r^2 (Figure 6b). The overall estimation accuracies are similar for both the pre-TGD and post-TGD periods, despite slightly lower mean bias and RMSE for the pre-TGD period and a higher r^2 for the post-TGD period.

floods in 2002 and 2010 [Shankman *et al.*, 2012] and the prevalent droughts in 2006 and 2011 (with a half-century minimum of spring precipitation in 2011) [Cai *et al.*, 2016; Wang *et al.*, 2014a], which are significantly correlated with the El Niño-Southern Oscillation (ENSO) [Z. Z. Zhang *et al.*, 2015]. Was such climate variability influential enough to lead to the YP lake decline that is poorly explained by direct human interventions?

To seek the answer, we simulate daily flows incorporating both anthropogenic and meteorological influences (*realistic* scenario), and test whether these flows can approach a thorough explanation of the observed post-TGD decline and decreasing trends in the natural lake system (refer back to section 4.4). Modeling lake areas from surface flows involves various uncertainties stemming from the complexity of river-lake hydrodynamics and inundation hysteresis (detailed model performance and uncertainty analysis given in supporting information). Despite these uncertainties, our estimated Class I lake areas, including the impacts of climate variability, TGD operation, and human water consumption, agree well with our remote sensing observations (Figure 6), and capture an average of 91.2% of the post-TGD decline and over 95% of the decreasing trends (Figure 5d and Solution 1 in Tables 2 and 3). The contribution of climate variation alone is then separated by the established flow-area model using flow simulations driven only by climate forcings (*pristine* scenario).

We reveal that climate variation across the downstream Yangtze Basin contributes an average of 87.0% of the post-TGD lake decline (i.e., 134.1% in winter, 66.9% in spring, 77.7% in summer, and 81.7% in fall) (Figure 4f and Table 2), and 90.7 (±17.2)% and 97.3 (±32.7)% of the decreasing trends during 2000–2011 and post-TGD periods, respectively (Figures 5c and 5d and Table 3). By testing these contributions with their estimation uncertainties, we infer a moderate to high confidence (with most probabilities ranging from 70% to over 90%) that the assessed climate impacts are statistically equivalent to the observed lake declines (Tables 2 and 3).

Since simulated *pristine* discharges reflect an integrated effect of various climate factors, we next compare the time series of mapped lake areas with precipitation and temperature separately, in order to obtain a qualitative understanding of which factor may be more responsible for the lake decline. As illustrated in supporting information Figure S2, the Yangtze Basin experienced a general decrease in precipitation but increase in temperature during 2000–2011. Precipitation appears to drive the overall lake dynamics, reflected by a significant positive correlation between lake area and precipitation (in both full time series and anomalies). The severe drought anomalies in 2006 and 2011, in particular, led to strikingly low lake areas, which are critical determinants to the decadal lake decline. At the same time, increasing temperature, which negatively correlates with lake area, tended to enhance evapotranspiration and reduce surface runoff, leading to a deteriorated drought in the lake system across the YP.

To further evaluate the combined human and climate impacts on the natural lake system, we aggregate the climate contribution to our quantified impacts of TGD's flow regulation, net channel erosion, and human water consumption (Solution 2 in Tables 2 and 3), as an alternative solution to the estimates directly using surface flows (Solution 1 as described above). In the latter, human impacts on lake inundation area are directly inferred from simulated flow changes rather than from calibrated Yangtze level changes induced by flow changes, and thus take no explicit account of the impact of Yangtze channel erosion. However, except minor

impact increments in Solution 2, both results are highly consistent, which account for over 91% of the observed post-TGD lake decline and explain almost completely the observed lake decreasing trends.

Due to strict floodgate management, the controlled (Class II) lakes in the YP exhibit a seasonal inundation pattern considerably different from the meteorological cycle (Figure 7); even so, their inundation area agrees closely with natural catchment water supply (r_q) on the annual time scale (Figure 7f). By aggregating the annual means of both natural and controlled lake areas (Figures 7b and 7f), we find a 0.97 rank correlation coefficient between the interannual dynamics of YP lake area and natural water supply, which further suggests a substantial role of local climate in driving the decadal area decline across the YP lake system.

Concurrent with the discussed factors, numerous reservoirs in the tributary catchments appear to have intensified water impoundments. This is manifested by, for example, the expanding area of 28 Class III lakes (i.e., major reservoirs in the downstream Yangtze Basin) in Figures 7i–7l [also see Wang *et al.*, 2014a] and the increasing total storage in 108 reservoirs bigger than 0.1 km³ across the entire Yangtze Basin by Cai *et al.* [2016]. Reservoir regulations downstream of the TGD cause additional interventions with tributary water supply to the YP lakes [Long *et al.*, 2015], and water impoundments in the upstream catchments may reduce the natural inflow to the TGD, which is not fully considered in our model simulations (refer back to section 4.1). Cai *et al.* [2016] concluded that during 2000–2014, TGR's water impoundment alone accounts for more than 80% of the storage increase in all 108 large reservoirs across the Yangtze Basin. The net storage increase in these reservoirs except the TGR is about 0.4 Gt yr⁻¹ [Cai *et al.*, 2016], equivalent to only 0.1% of the annual Yangtze flow entering the downstream basin. By adding middle-sized and small reservoirs, Yang *et al.* [2015] showed that the total water storage in all reservoirs across the Yangtze Basin, including their surface evaporative loss, probably increased by ~9.5 Gt yr⁻¹ during 2000–2011, which is equivalent to ~2.4% reduction of the Yangtze flow to the downstream basin and about ~1.7 times greater than TGD's flow regulation. Inferred from the limited impact of TGD's flow regulation we have quantified, the aggregated contribution of the other reservoirs to the YP lake decline (at least for Class I) is likely below ~5%.

If we assume that half of the water storage increase in all reservoir except the TGR occurred in the upstream Yangtze Basin, this will reduce the Yangtze flow to the downstream basin by less than ~1%. This miniscule influence also supports our previous assumption that the observed trend in TGD inflow is largely attributed to upstream climate variation. More corroborations are suggested in (i) supporting information Figure S4, which shows a fairly good agreement between our simulated natural flows and observed TGD inflows and (ii) another modeling study by Birkinshaw *et al.* [2016], which applied the hydrological model SHETRAN with station climate data observed in the upstream Yangtze Basin to obtain an excellent match between simulated and measured flows before 2006 immediately downstream of the TGD.

Our assessments do not take into account a range of other anthropogenic factors such as urbanization, afforestation, and sand dredging, which may be responsible for our estimation uncertainties and the remaining gap in our unexplained lake area decline. For instance, several studies [Feng *et al.*, 2011b; Jiang *et al.*, 2015; X. J. Lai *et al.*, 2014; Sun *et al.*, 2012; Xu and Milliman, 2009; Yang *et al.*, 2014] imply that intensive sand dredging during our study period has led to detectable lake bathymetrical changes, which could negatively affect lake inundation area (e.g., about -0.6% yr⁻¹ for Lake Poyang as we verify in supporting information Figure S7).

As some studies [e.g., Feng *et al.*, 2013; Wang, 2013] have questioned, altered lake area by the TGD changed the supply of open water evaporation, which may have in turn affected the local climate and thus the downstream lake area. Nevertheless, given an average TGD impact of less than ~4% in concurrent lake area or ~3% in lake area seasonality (Figure 4), the speculated influence on the downstream climate, particularly compared to the scale of ENSO variability, is likely limited or even negligible. Therefore, we conclude that the observed decadal lake decline across the YP is a primary consequence of local climate variability, rather than direct anthropogenic interventions.

5.4. Outlook for the Yangtze Lake System Under a Fully Operational TGD

We have shown that the dominant driver of the recent Yangtze lake dynamics stems from climate variation; however, human water regulation and consumption exert persistent impacts on lake inundation, and thus remain important factors to lake management and conservation. Starting in the fall of 2008, the TGR attempted the final pilot impoundment and eventually reached its designed ultimate water level (175 m asl) in October 2010 [China Three Gorges Construction Yearbook Commission, 2011; Ou *et al.*, 2012; Wang

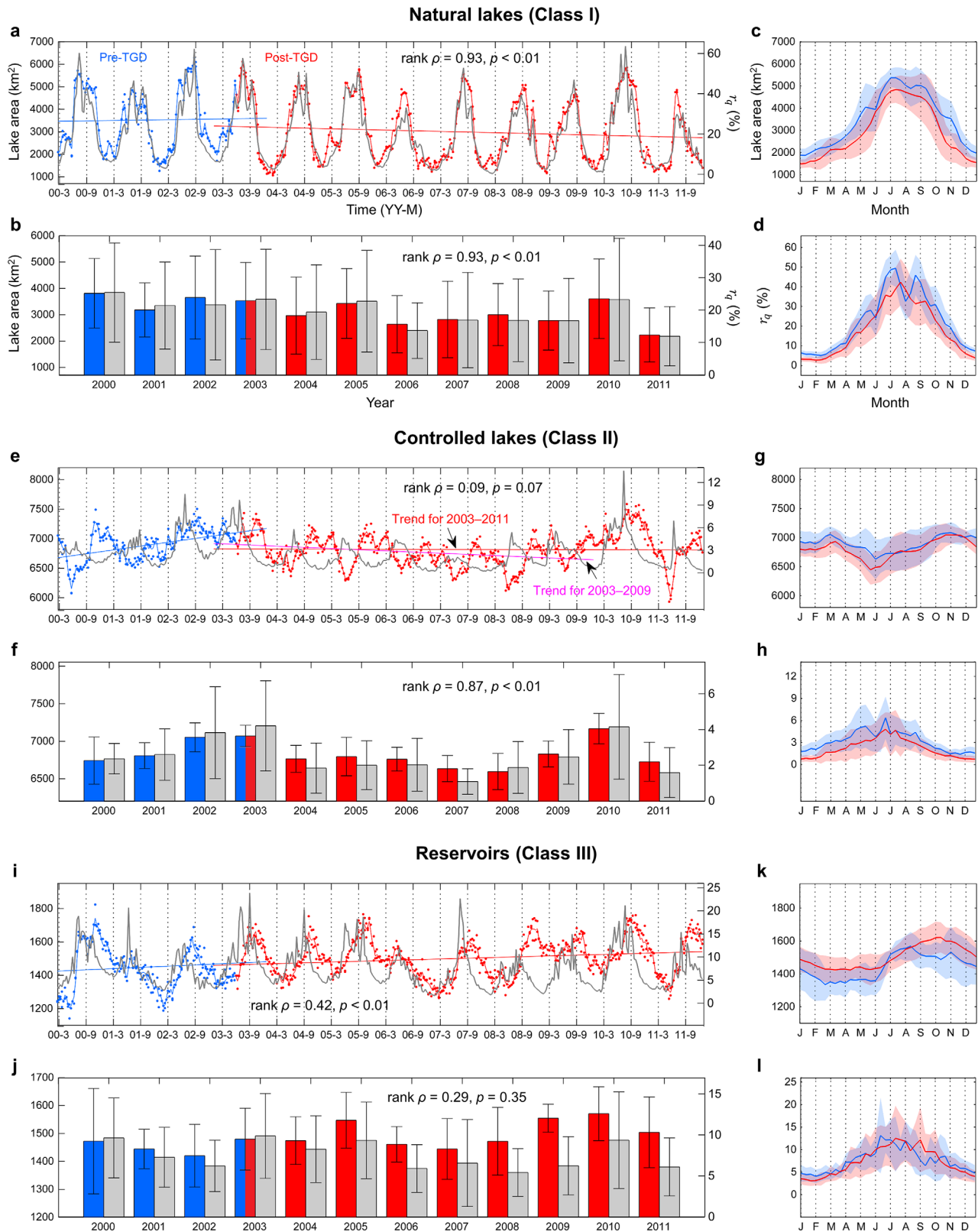


Figure 7. Comparisons of observed lake inundation area and simulated natural water supply. (a–d) Class I. (e–h) Class II. (i–l) Class III. (left) Interannual dynamics in 10 day series (Figures 7a, 7e, and 7i) and annual means (Figures 7b, 7f, and 7j). (right) Annual mean cycles. Axis labels for Classes II and III are consistent with those for Class I. Blue and red: pre-TGD and post-TGD periods, respectively. Grey: natural relative discharge (r_q) (see definition in section 4.4.2). Calculation of r_q for Class I lakes follows the same method for Classes II and III (equation (12)), except that Class I q_n is the lake-Yangtze confluence flow in order to include the Yangtze River impact on the lake boundary condition. The climate dominance on Class I is further supported by the significant agreement between lake area and r_q on both 10 day and annual time scales (Spearman's rank $\rho=0.93$, $p < 0.01$ (Figure 7a)), which is consistent with the agreement between lake area and precipitation in supporting information Figure S2. Intraannual patterns of Class II and III areas are discrepant from those of r_q (Figures 7e, 7g–7i, and 7k–7l), implying substantial seasonal human control. Class II area, however, agrees well with r_q on the annual time scale ($\rho=0.87$, $p < 0.01$ (Figure 7f)), suggesting a dominant climate impact on the general interannual after trend. This is similarly supported by the phase drop in mean annual cycles of both lake area (Figure 7g) and r_q (Figure 7h) despite their opposite seasonal patterns. Different from the YP lakes, Class III area shows a significant interannual increase, contrasting with the general decrease in r_q (Figures 7i–7l). This contrast implies intensified human water regulations in these tributary reservoirs, which may reduce downstream water supply and contribute to the YP lake decline.

et al., 2013]. The downstream Yangtze regime has since been regulated under TGD's full-capacity water dispatch scheme. To discern the maximal influence of TGD's water regulation, we summarize the mean annual cycles of aggregated lake area across the YP during 2009–2011 (Figures 8a–8d). The revealed intraannual impacts are generally double to triple the influences averaged in the studied post-TGD period (see statistics including seasonal impacts on major natural lakes, Poyang and Dongting, in supporting information Table S8). The total lake inundation area across the YP is increased by up to 2.7% in winter and spring, and decreased by 0.1–6.5% in fall. The natural processes of lake seasonal growth and recession are accelerated, i.e., by approximately 5–10 days in spring and 15–25 days in fall, respectively, and the lake area stabilized by 19.8% in summer. As an overall outcome of TGD's full-capacity regulation, the seasonal variation of YP lake inundation area is slightly reduced by 4.9% with a negligible impact on the annual mean ($0.1 (\pm 2.1)\%$).

Although the TGD has currently reached its full regulation, downstream Yangtze channel erosion remains a chronic process [Yang *et al.*, 2006, 2014]. As of 2009–2011, the net channel erosion had counteracted 48.7% and 30.5% of the lake area increase expected by TGD's full water dispatches in winter and spring, respectively, and reinforced 14.1% of the lake drainage in fall (Figure 8d). As channel erosion continues in the next four to five decades or so [Yang *et al.*, 2006], its negative impact will be further amplified and thus increasingly critical to the surrounding lake and wetland system. By simply applying the regulated Yangtze flows in 2009–2011 to the channel geometry in 2012, we observe slightly additional lake decline (supporting information Figure S8) as a result of ongoing channel incision even during a period of 1–3 years.

The effect of future climate on the Yangtze Basin is still uncertain [Birkinshaw *et al.*, 2016; Gu *et al.*, 2015; Liu *et al.*, 2008; Schewe *et al.*, 2014; Shankman *et al.*, 2012], but local and transbasin water consumptions, which are major anthropogenic inducers of hydrological drought [Wada *et al.*, 2013], may likely increase with rising water demand from population growth, economic expansion, and living standard improvement in the coming decade(s) [Wada *et al.*, 2014a; Zhao *et al.*, 2007; Erzin and Hoekstra, 2014; Jiang, 2009]. During 2009–2011, human water consumption led to an annual reduction of $79.6 (\pm 52.4)$ km² or $3.0 (\pm 1.9)\%$ of the total inundation area in the natural lakes (Figures 8e–8h). The seasonal reduction already accounts for 30.6% of TGD's full water storage effect in fall and almost completely offsets the benefit of TGD's water release in winter (by 96.4%). As we suggest, climate variability may likely drive the overall lake dynamics in the near future; however, if the impacts of human water consumption and Yangtze channel erosion continuously strengthen and exceed the constraint of TGD's flow regulation, anthropogenic influences will only become more important to the critical lake systems across the YP.

6. Discussion and Concluding Remarks

Our results reveal an overdue explanation of the recent decadal lake decline in the YP through quantitative attributions to major anthropogenic factors (i.e., the TGD and human water consumption) and climate variability. We conclude that direct human activities are not a primary cause of this decline; neither can TGD-induced lake area changes likely alter the regional climate variability which we estimate to be the dominant factor triggering the observed lake decline. Despite a different focus, our overall conclusion is consistent with the recent finding from Yang *et al.* [2015] that climate variability explains most of the decrease of Yangtze River flow in the post-TGD decade compared to a longer pre-TGD period from 1950s.

Several limitations may be addressed in future improvements. First, we focus on the changes in inundation area, rather than water storage, in selected major lake regions accounting for +85% of the total YP lakes in both area and storage (volume estimated from the HydroLAKES dataset [Messenger *et al.*, 2016]). However, since TGD's impacts on lake inundation area are small, we speculate that its impacts on the total lake water storage across the YP are likely limited as well. Second, our assessed anthropogenic factors exclude water regulations in tributary reservoirs, land cover land use changes, and lake bathymetric alterations, although their integrated impact is somewhat implied by lake area changes unexplained by our studied factors. Third, our conclusion of the climate dominance on the YP lake changes is based on the assumption that recent human activities in the upstream Yangtze Basin do not alter the intrinsic trend in TGD inflow, which is generally corroborated by our analysis and existing literature. Fourth, we emphasize direct human impacts on the Yangtze hydrological regime, which do not include human-induced climate change. A more thorough separation between natural and human impacts requires a better understanding of how recent climate variation is coupled with, and possibly induced by, other anthropogenic forcing in broader and longer contexts.

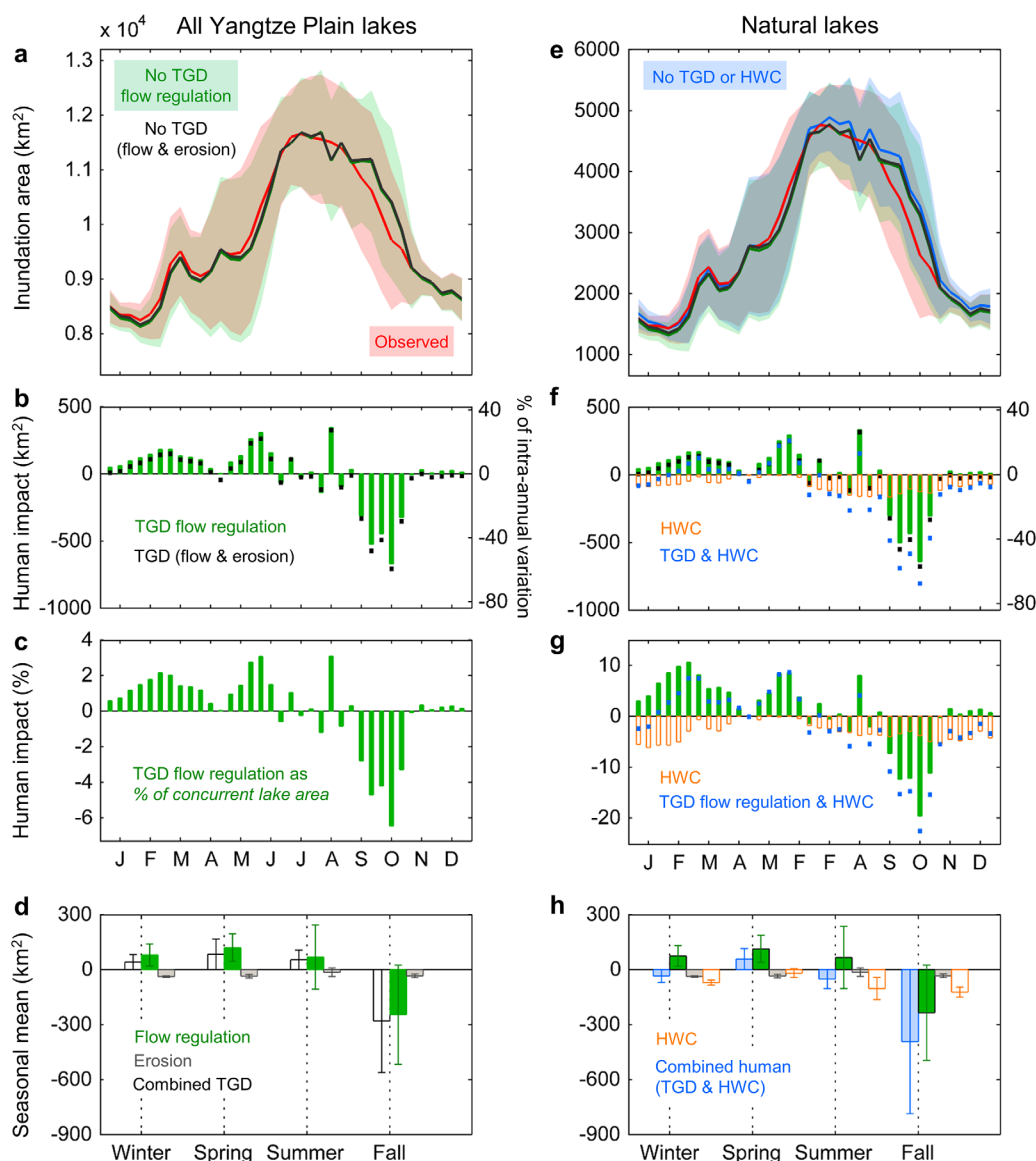


Figure 8. Anthropogenic impacts on intraannual lake area variation during the TGD full-operation period (2009–2011). Illustration of impacts on (left) (a–d) all YP lakes and (right) (e–h) natural lakes alone. (a, e) Ten day mean annual cycles of observed and modeled lake areas (shaded areas illustrate lake area standard deviations). (b, f) Ten day mean annual cycles of human-induced lake area changes (left axis) and those changes as percentages of the intraannual lake area variation without TGD’s flow regulation (right axis). (c, g) Ten day mean annual cycles of human-induced lake area changes as percentages of concurrent lake areas without TGD’s flow regulation. (d, h) Seasonal means of all studied human impacts (error bars illustrate standard deviations of assessed impacts within each season).

In addition, our applied hydrological model, PCR-GLOBWB [van Beek et al., 2011; Wada et al., 2014b, 2016, 2011a, 2011b], although being widely accepted in both global and regional studies, has inevitable limitations in routing scheme and parameter regionalization [Weiland et al., 2015], and our discharge simulations are forced only by the ERA-Interim reanalysis climate data. To remedy some of these limitations, we calibrate simulated streamflow using gauging measurements (for assessing human impacts), evaluate modeled lake inundation areas against remote sensing observations, and quantify multiple uncertainties to infer confidence intervals for all estimates. Future work using multimodel ensemble and observed climate data may be necessary to verify and hopefully further secure our primary conclusions.

Despite an emphasis on disaggregating anthropogenic and climate factors, our results also signify that anthropogenic impacts are nontrivial on the seasonal scale and have strengthened persistently over the past decade. In particular, the expedited lake drainage due to TGD’s increasing water storage, which is

observable by gravimetric satellites [Long et al., 2015; Long et al., 2017], leads to ~40% acceleration of the climate-induced lake decrease in fall. Although TGD's full water regulation (since 2009) alters only marginal portions (less than 6.5%) of the total YP lake area, its seasonal impacts, including water drainage in fall and submergence in winter and spring, become amplified (up to ~10–20%) when examined on individual natural lakes such as Dongting and Poyang (supporting information Table S8). Such greater regional impacts call for immediate adaptation to the disturbed submerging pattern (e.g., reevaluation of the newly proposed Poyang Lake Dam) [Jiao, 2009] in order to better protect the vital wetland ecosystems that still remain naturally connected to the Yangtze River.

As we show, the negative impacts of Yangtze channel erosion and human water consumption are comparable to that of TGD's water regulation. This is so even though our estimates are validated to be conservative and we take no account of water consumption in the upstream Yangtze Basin or lake bathymetric changes due to expedited water drainage, sediment mining, and tributary damming [Feng et al., 2011b; Jiang et al., 2015; X. J. Lai et al., 2014]. Growth of these impacts likely proceeds regardless of TGD's full water regulation, particularly considering (i) the ongoing boom in dam construction across the Yangtze Basin [Zarfl et al., 2015] which continues exacerbating downstream sediment deficiency and (ii) the recently initiated South-to-North Water Transfer/Diversion Project (Liu et al., 2013; Office of the South-to-North Water Diversion Project Commission of the State Council data are available at www.nsb.gov.cn/zh/english) allowing additional water and sediment loss via transbasin transfer [Yang et al., 2002].

Increasing human impacts accompany future climate uncertainties in the Yangtze Basin. Our study period ends in the dry anomaly year of 2011, which was followed by higher precipitation and continuously rising temperature during 2012–2016 (supporting information Figure S2). Despite a partial alleviation from the precipitation, significant declining trends in both YP lake area and storage persisted till at least 2014 [Cai et al., 2016]. The future stability and integrity of the YP lake system will largely depend on the frequency and intensity of climate anomalies, which are broadly related to the ENSO modulation. To this end, we foresee the necessity of future lake conservation efforts, by seeking optimized coordination among water regulation, consumption, and diversion under projected climate change and socioeconomic development within and beyond the Yangtze Basin.

Appendix A: List of Variable and Function Notations

Symbol	Definition
A	Lake area mapped from MODIS imagery
a	Lake area under the <i>realistic</i> scenario (see Table 1 for all model scenarios)
a_c	Lake area under the <i>consumed</i> scenario
$a_{c'}$	Similar to a_c but under human water consumption during the pre-TGD period
a_n	Lake area under the <i>pristine</i> scenario
a_r	Lake area under the <i>regulated</i> scenario
a_u	Lake area under the <i>unregulated</i> scenario
Δa_c	Lake area change induced by human water consumption
Δa_e	Lake area change induced by net channel erosion
Δa_r	Lake area change induced by TGD's flow regulation
L	In situ Yangtze level
L^*	Yangtze level at surrogate station
l	Lake outlet level under the <i>realistic</i> scenario
l_c	Lake outlet level under the <i>consumed</i> scenario
l_n	Lake outlet level under the <i>pristine</i> scenario
l_r	Lake outlet level under the <i>regulated</i> scenario
l_u	Lake outlet level under the <i>unregulated</i> scenario
Q	In situ Yangtze flow
q	Yangtze flow under the <i>realistic</i> scenario
q^*	Yangtze flow under the <i>realistic</i> scenario at surrogate station
q'	Lake catchment flow under the <i>realistic</i> scenario
q_c	Yangtze flow under the <i>consumed</i> scenario ($q_c \equiv q_u$)
q_n	Yangtze flow under the <i>pristine</i> scenario
q_r	Yangtze flow under the <i>regulated</i> scenario
q_u	Yangtze flow under the <i>unregulated</i> scenario ($q_u = Q - \Delta q_r$)
Δq_c	Flow change induced by human water consumption

(continued)

Appendix (continued)

Symbol	Definition
$\Delta q_{\Delta c}$	Net change of Δq_c between the pre-TGD and post-TGD periods
Δq_r	Yangtze flow changes induced by TGD's water regulation ($\Delta q_r = q_r - q_n$)
r_q	Relative discharge (see equation (12))
s_q	Standardized discharge (see equation (12))
ϕ_y	Stage-discharge rating curve in year y
ϕ_y^{-1}	Inverse stage-discharge rating curve in year y
ϕ_0	Stage-discharge rating curve in the benchmark year 2004
η	Empirical relation between lake area (A) and outlet level (L)
ψ	Empirical relation between lake area (A) and confluence flow (q)
ξ	Empirical relation between residual in ψ and lake catchment flow (q')

Acknowledgments

This study was supported by the United States Geological Survey (USGS) Landsat Science Team Program Grant (G12PC00071), University of California Dissertation Year Fellowship, and Kansas State University faculty start-up fund. Hongzhao Zang (University of Southern California) and Ruishan Chen (East China Normal University) provided generous help in acquiring gauging data and water resources bulletins. Constructive suggestions and discussions were provided by Chunqiao Song, Colin J. Gleason, Laurence C. Smith, Tak Shun D. Tong, Kang Yang, Steven A. Margulis, Vena W. Chu, Shenyue Jia and Michael E. Shin (UCLA), Jordan M. McAlister (Oklahoma State University), Junli Li (Xinjiang Institute of Geography and Ecology, Chinese Academy of Sciences), Xianwei Wang (Sun Yat-sen University, China), and Richard A. Marston, Lei Luo, and Fangfang Yao (Kansas State University). We are indebted to the Associated Editor, the Editor, and four anonymous reviewers for their extremely valuable insights and suggestions. We also acknowledge the NOAA/OAR/ESRL PSD (Boulder, Colorado) for providing meteorological datasets (CMAP, CRUTEM4v, NOAAGlobalTemp, and PREC/L) through their website at www.esrl.noaa.gov/psd. No major financial conflicts of interests are identified. Produced lake extent shapefiles mapped from MODIS daily imagery in the downstream Yangtze Basin are accessible online in the PANGAEA database (<https://doi.pangaea.de/10.1594/PANGAEA.841056>). All analytical codes are available upon request.

References

- Balsamo, G., S. Boussetta, P. Lopez, and L. Ferranti (2010), *Evaluation of ERA-Interim and ERA-Interim-GPCP-Rescaled Precipitation Over the U.S.A.*, *ERA Rep. Ser. 5*, 10 pp., Eur. Cent. for Medium-Range Weather Forecasts, Reading, U. K.
- Berkeley Earth (2017), *Monthly Land Average Temperature* (TAVG; 1753 – Recent). [Available at http://berkeleyearth.lbl.gov/auto/Global/Gridded/Complete_TAVG_LatLong1.nc.]
- Birkinshaw, S. J., S. B. Guerreiro, A. Nicholson, Q. Liang, P. Quinn, L. Zhang, B. He, J. Yin, and H. J. Fowler (2016), Climate change impacts on Yangtze River discharge at the Three Gorges Dam, *Hydrol. Earth Syst. Sci.*, *21*, 1911–1927, doi:10.5194/hess-2016-231.
- Cai, X. B., L. Feng, X. J. Hou, and X. L. Chen (2016), Remote sensing of the water storage dynamics of large lakes and reservoirs in the Yangtze River Basin from 2000 to 2014, *Sci. Rep.*, *6*, 36405, doi:10.1038/srep36405.
- Changjiang Water Resources Commission (2000–2011), *Changjiang and southwest rivers water resources bulletin* [in Chinese], Yangtze River Publishing House, Wuhan, Hubei, China. [Available at <http://www.cjw.gov.cn/zwzc/bmgb>, accessed on Nov 01 2014.]
- Chen, L., R. Michishita, and B. Xu (2014), Abrupt spatiotemporal land and water changes and their potential drivers in Poyang Lake, 2000–2012, *ISPRS J. Photogramm. Remote Sens.*, *98*, 85–93.
- Chen, M. Y., P. P. Xie, J. E. Janowiak, and P. A. Arkin (2002), Global land precipitation: A 50-yr monthly analysis based on gauge observations, *J. Hydrometeorol.*, *3*(3), 249–266.
- China Three Gorges Construction Yearbook Commission (2004), *Three Gorges Construction Yearbook 2004* [in Chinese], pp. 401, Publisher of China Three Gorges Construction Yearbook, Yichang, Hubei, China.
- China Three Gorges Construction Yearbook Commission (2011), *Three Gorges Construction Yearbook 2011* [in Chinese], pp. 309, Publisher of China Three Gorges Construction Yearbook, Yichang, Hubei, China.
- Crutzen, P. J. (2002), Geology of mankind, *Nature*, *415*(6867), 23–23.
- Dai, S. B., S. L. Yang, J. Zhu, A. Gao, and P. Li (2005), The role of Lake Dongting in regulating the sediment budget of the Yangtze River, *Hydrol. Earth Syst. Sci.*, *9*(6), 692–698.
- Dai, X., R. R. Wan, and G. S. Yang (2015), Non-stationary water-level fluctuation in China's Poyang Lake and its interactions with Yangtze River, *J. Geogr. Sci.*, *25*(3), 274–288.
- Dai, Z. J., and J. T. Liu (2013), Impacts of large dams on downstream fluvial sedimentation: An example of the Three Gorges Dam (TGD) on the Changjiang (Yangtze River), *J. Hydrol.*, *480*, 10–18.
- Dee, D. P., et al. (2011), The ERA-Interim reanalysis: Configuration and performance of the data assimilation system, *Q. J. R. Meteorol. Soc.*, *137*(656), 553–597.
- Ding, X. W., and X. F. Li (2011), Monitoring of the water-area variations of Lake Dongting in China with ENVISAT ASAR images, *Int. J. Appl. Earth Obs. Geoinf.*, *13*(6), 894–901.
- Du, Y., H. P. Xue, S. J. Wu, F. Ling, F. Xiao, and X. H. Wei (2011), Lake area changes in the middle Yangtze region of China over the 20th century, *J. Environ. Manage.*, *92*(4), 1248–1255.
- Ercin, A. E. and A. Y. Hoekstra (2014), Water footprint scenarios for 2050: A global analysis, *Environ. Int.*, *64*, 71–82.
- Fang, J., S. Rao, and S. Zhao (2005), Human-induced long-term changes in the lakes of the Jiangnan Plain, Central Yangtze, *Frontiers Ecol. Environ.*, *3*(4), 186–192.
- Feng, L., C. M. Hu, X. L. Chen, and R. F. Li (2011a), Satellite observations make it possible to estimate Poyang Lake's water budget, *Environ. Res. Lett.*, *6*(4), 044023.
- Feng, L., C. M. Hu, X. L. Chen, R. F. Li, L. Q. Tian, and B. Murch (2011b), MODIS observations of the bottom topography and its inter-annual variability of Poyang Lake, *Remote Sens. Environ.*, *115*(10), 2729–2741.
- Feng, L., C. M. Hu, and X. L. Chen (2012a), Satellites capture the drought severity around China's largest freshwater lake, *IEEE J. Sel. Top. Appl. Earth Obs. Remote Sens.*, *5*(4), 1266–1271.
- Feng, L., C. M. Hu, X. L. Chen, X. B. Cai, L. Q. Tian, and W. X. Gan (2012b), Assessment of inundation changes of Poyang Lake using MODIS observations between 2000 and 2010, *Remote Sens. Environ.*, *121*, 80–92.
- Feng, L., C. Hu, X. Chen, and X. Zhao (2013), Dramatic inundation changes of China's two largest freshwater lakes linked to the Three Gorges Dam, *Environ. Sci. Technol.*, *47*(17), 9628–9634.
- Gao, J. H., et al. (2014), Changes in water and sediment exchange between the Changjiang River and Poyang Lake under natural and anthropogenic conditions, China, *Sci. Total Environ.*, *481*, 542–553.
- GISTEMP Team (2017), *GISS Surface Temperature Analysis (GISTEMP) Data Set*, NASA Goddard Inst. for Space Stud., New York, N. Y. [Available at data.giss.nasa.gov/gistemp/.]
- Gleick, P. H., H. Cooley, M. J. Cohen, M. Morikawa, J. Morrison, and M. Palaniappan (2009), *The World's Water 2008–2009: The Biennial Report on Freshwater Resources*, Island Press, Washington, D. C.
- Gu, H. H., Z. B. Yu, G. L. Wang, J. G. Wang, Q. Ju, C. G. Yang, and C. H. Fan (2015), Impact of climate change on hydrological extremes in the Yangtze River Basin, China, *Stochastic Environ. Res. Risk Assess.*, *29*(3), 693–707.

- Guo, H., Q. Hu, Q. Zhang, and S. Feng (2012), Effects of the Three Gorges Dam on Yangtze River flow and river interaction with Poyang Lake, China: 2003–2008, *J. Hydrol.*, *416*, 19–27.
- Hansen, J., R. Ruedy, M. Sato, and K. Lo (2010), Global surface temperature change, *Rev. Geophys.*, *48*, RG4004, doi:10.1029/2010RG000345.
- Huang, Q., Z. Sun, and J. Jiang (2011), Impacts of the operation of the Three Gorges Reservoir on the lake water level of Lake Dongting, *Hupo Kexue*, *23*(3), 424–428.
- Huang, Q., Z. Sun, C. Opp, T. Lotz, J. Jiang, and X. Lai (2014), Hydrological drought at Dongting Lake: Its detection, characterization, and challenges associated with Three Gorges Dam in Central Yangtze, China, *Water Resour. Manage.*, *28*(15), 5377–5388.
- Huang, S. F., J. G. Li, and M. Xu (2012), Water surface variations monitoring and flood hazard analysis in Dongting Lake area using long-term Terra/MODIS data time series, *Nat. Hazards*, *62*(1), 93–100.
- Huang, Y., S. Chen, H. Wu, and M. Zhu (2007), Analysis of evolution factors and ecological protection strategies for Honghu Lake, *Resour. Environ. Yangtze Basin*, *16*(4), 504–508.
- Huffman, G. J., R. F. Adler, D. T. Bolvin, G. J. Gu, E. J. Nelkin, K. P. Bowman, Y. Hong, E. F. Stocker, and D. B. Wolff (2007), The TRMM multisatellite precipitation analysis (TMPA): Quasi-global, multiyear, combined-sensor precipitation estimates at fine scales, *J. Hydrometeorol.*, *8*(1), 38–55.
- Jiang, F., S. Qi, F. Liao, X. Zhang, D. Wang, J. Zhu, and M. Xiong (2015), Hydrological and sediment effects from sand mining in Poyang Lake during 2001–2010, *Acta Geogr. Sin.*, *70*(5), 837–845.
- Jiang, Y. (2009), China's water scarcity, *J. Environ. Manage.*, *90*(11), 3185–3196.
- Jiao, L. (2009), CHINA Scientists line up against dam that would alter protected wetlands, *Science*, *326*(5952), 508–509.
- Jones, P. D., D. H. Lister, T. J. Osborn, C. Harpham, M. Salmon, and C. P. Morice (2012), Hemispheric and large-scale land-surface air temperature variations: An extensive revision and an update to 2010, *J. Geophys. Res.*, *117*, D05127, doi:10.1029/2011JD017139.
- Klein Goldewijk, K., and G. van Drecht (2006), HYDE 3: Current and historical population and land cover, in *Integrated Modelling of Global Environmental Change: An Overview of IMAGE 2.4*, edited by A. F. Bouwman, T. Kram, and K. Klein Goldewijk, pp. 93–112, Neth. Environ. Assess. Agency (MNP), Bilthoven, Netherlands.
- Lai, X., J. Jiang, and Q. Huang (2013a), Effects of the normal operation of the Three Gorges Reservoir on wetland inundation in Dongting Lake, China: A modelling study, *Hydrol. Sci. J.*, *58*(7), 1467–1477.
- Lai, X., J. Jiang, Q. Liang, and Q. Huang (2013b), Large-scale hydrodynamic modeling of the middle Yangtze River Basin with complex river-lake interactions, *J. Hydrol.*, *492*, 228–243.
- Lai, X., Q. Liang, J. Jiang, and Q. Huang (2014), Impoundment effects of the Three-Gorges-Dam on flow regimes in two China's largest freshwater lakes, *Water Resour. Manage.*, *28*(14), 5111–5124.
- Lai, X. J., D. Shankman, C. Huber, H. Yesou, Q. Huang, and J. H. Jiang (2014), Sand mining and increasing Poyang Lake's discharge ability: A reassessment of causes for lake decline in China, *J. Hydrol.*, *519*, 1698–1706.
- Lehner, B., et al. (2011a), *Global Reservoir and Dam Database, Version 1 (GRanDv1): Reservoirs, Revision 01*, NASA Socioecon. Data and Appl. Cent., Palisades, N. Y., doi:10.7927/H4HH6H08.
- Lehner, B., et al. (2011b), High-resolution mapping of the world's reservoirs and dams for sustainable river-flow management, *Frontiers Ecol. Environ.*, *9*(9), 494–502.
- Leopold, L. B., and T. Maddock (1953), The hydraulic geometry of stream channels and some physiographic implications, *U.S. Geol. Surv. Prof. Pap.*, *252*, 64 pp.
- Li, X., and Q. Zhang (2014), Variation of floods characteristics and their responses to climate and human activities in Poyang Lake, China, *Chin. Geogr. Sci.*, *25*(1), 13–25.
- Liu, B., T. Jiang, G. Ren, and F. Klaus (2008), Projected surface water resource of the Yangtze River Basin before 2050, *Adv. Clim. Change Res.*, *4*(3), 145–150.
- Liu, Y., and G. Wu (2014), Hydroclimatological influences at multi-spatial scales on recently increased droughts in China's largest freshwater lake, *Hydrol. Earth Syst. Sci. Discuss.*, *11*, 5633–5661.
- Liu, Y., G. Wu, and X. Zhao (2013), Recent declines in China's largest freshwater lake: Trend or regime shift?, *Environ. Res. Lett.*, *8*(1), 014010.
- Liu, J., C. Zang, S. Tian, J. Liu, H. Yang, S. Jia, L. You, B. Liu, and M. Zhang (2013), Water conservancy projects in China: Achievements, challenges and way forward, *Glob. Environ. Change*, *23*(3), 633–643.
- Long, D., Y. T. Yang, Y. Wada, Y. Hong, W. Liang, Y. N. Chen, B. Yong, A. Z. Hou, J. F. Wei, and L. Chen (2015), Deriving scaling factors using a global hydrological model to restore GRACE total water storage changes for China's Yangtze River Basin, *Remote Sens. Environ.*, *168*, 177–193.
- Long, D., Y. Pan, J. Zhou, Y. Chen, X. Hou, Y. Hong, B. R. Scanlon, and L. Longuevergne (2017), Global analysis of spatiotemporal variability in merged total water storage changes using multiple GRACE products and global hydrological models, *Remote Sens. Environ.*, *192*, 198–216.
- Lyons, E. A., Y. Sheng, L. C. Smith, J. Li, K. M. Hinkel, J. D. Lenters, and J. Wang (2013), Quantifying sources of error in multitemporal multi-sensor lake mapping, *Int. J. Remote Sens.*, *34*(22), 7887–7905.
- Ma, L., T. Zhang, O. W. Frauenfeld, B. Ye, D. Yang, and D. Qin (2009), Evaluation of precipitation from the ERA-40, NCEP-1, and NCEP-2 Reanalyses and CMAP-1, CMAP-2, and GPCP-2 with ground-based measurements in China, *J. Geophys. Res. Atmos.*, *114*, D09105, doi:10.1029/2008JD011178.
- Ma, R. H., H. T. Duan, C. M. Hu, X. Z. Feng, A. N. Li, W. M. Ju, J. H. Jiang, and G. S. Yang (2010), A half-century of changes in China's lakes: Global warming or human influence?, *Geophys. Res. Lett.*, *37*, L24106, doi:10.1029/2010GL045514.
- Ma, W., G. Yang, X. Wang, N. Qin, and X. Dai (2014), Progress of research on the relationship between the Yangtze River and its connected lakes in the middle reaches, *J. Lake Sci.*, *26*(1), 1–8.
- Messenger, M. L., B. Lehner, G. Grill, I. Nedeva, and O. Schmitt (2016), Estimating the volume and age of water stored in global lakes using a geo-statistical approach, *Nat. Commun.*, *13603*, doi: 10.1038/ncomms13603.
- Nilsson, C., C. A. Reidy, M. Dynesius, and C. Revenga (2005), Fragmentation and flow regulation of the world's large river systems, *Science*, *308*(5720), 405–408.
- Oak Ridge National Laboratory (2008), *LandScan High Resolution Global Population Data Set*, Oak Ridge, Tenn. [Available at web.ornl.gov/sci/landscan.]
- Ou, C. M., J. B. Li, Z. Q. Zhang, X. C. Li, G. Yu, and X. H. Liao (2012), Effects of the dispatch modes of the Three Gorges Reservoir on the water regimes in the Dongting Lake area in typical years, *J. Geogr. Sci.*, *22*(4), 594–608.
- Portmann, F. T., S. Siebert, and P. Doell (2010), MIRCA2000—Global monthly irrigated and rainfed crop areas around the year 2000: A new high-resolution data set for agricultural and hydrological modeling, *Global Biogeochem. Cycles*, *24*, GB1011, doi:10.1029/2008GB003435.
- Qiu, J. (2011), China admits problems with Three Gorges Dam, *Nature*, 25 May, doi:10.1038/news.2011.315.

- Rodell, M., H. K. Beaudoin, and NASA/GSFC/HSL (2016), *GLDAS Noah Land Surface Model L4 monthly 1.0 × 1.0 degree V2.1*, Goddard Earth Sci. Data and Inf. Serv. Cent., Greenbelt, Md. [Available at disc.sci.gsfc.nasa.gov/datacollection/GLDAS_NOAH10_M_V2.1.html].
- Rohwer, J., D. Gerten, and W. Lucht (2007), Development of functional types of irrigation for improved global crop modelling, *PIK Rep.* 104, 98 pp., Potsdam Inst. for Clim. Impact Res., Potsdam, Germany.
- Schewe, J., et al. (2014), Multimodel assessment of water scarcity under climate change, *Proc. Natl. Acad. Sci. U. S. A.*, 111(9), 3245–3250.
- Schneider, U., A. Becker, P. Finger, A. Meyer-Christoffer, B. Rudolf, and M. Ziese (2011), *GPCC Full Data Reanalysis Version 7.0 at 0.5°: Monthly Land-Surface Precipitation From Rain-Gauges Built on GTS-Based and Historic Data*, The NOAA/OAR/ESRL PSD, Boulder, Colo., doi:10.5676/DWD_GPCC/FD_M_V7_050. [Available at www.esrl.noaa.gov/psd/data/gridded/data.gpcc.html].
- Shankman, D., B. D. Keim, T. Nakayama, R. F. Li, D. Y. Wu, and W. C. Remington (2012), Hydroclimate analysis of severe floods in China's Poyang Lake region, *Earth Interact.*, 16, 1–16, doi:10.1175/2012EI000455.
- Shiklomanov, I. A. (Ed.) (1997), *Assessment of Water Resources and Water Availability in the World: Comprehensive Assessment of the Freshwater Resources of the World*, World Meteorol. Org., Geneva.
- Siebert, S., and P. Doell (2010), Quantifying blue and green virtual water contents in global crop production as well as potential production losses without irrigation, *J. Hydrol.*, 384(3–4), 198–217.
- Steinfeld, H., P. Gerber, T. Wassenaar, V. Castel, M. Rosales, and C. de Haan (2006), *Livestock's long shadow: Environmental issues and options*, report, 390 pp., Food and Agric. Org. of the U. N., Rome, Italy.
- Sun, F. D., Y. Y. Zhao, P. Gong, R. H. Ma, and Y. J. Dai (2014), Monitoring dynamic changes of global land cover types: Fluctuations of major lakes in China every 8 days during 2000–2010, *Chin. Sci. Bull.*, 59(2), 171–189.
- Sun, Z. D., Q. Huang, C. Opp, T. Hennig, and U. Marold (2012), Impacts and implications of major changes caused by the Three Gorges Dam in the middle reaches of the Yangtze River, China, *Water Resour. Manage.*, 26(12), 3367–3378.
- SWBD (2005), Shuttle Radar Topography Mission Water Body Data set. [Available at <http://www2.jpl.nasa.gov/srtm/index.html>].
- Szczypta, C., J. C. Calvet, C. Albergel, G. Balsamo, S. Boussetta, D. Carrer, S. Lafont, and C. Meurey (2011), Verification of the new ECMWF ERA-Interim reanalysis over France, *Hydrol. Earth Syst. Sci.*, 15(2), 647–666.
- Theil, H. (1950), A rank-invariant method of linear and polynomial regression analysis, 1, 2, and 3, *Ned. Akad. Wet. Proc.*, 53, 386–392, 521–525, 1397–1412.
- van Beek, L. P. H., Y. Wada, and M. F. P. Bierkens (2011), Global monthly water stress: 1. Water balance and water availability, *Water Resour. Res.*, 47, W07517, doi:10.1029/2010WR009791.
- Vörösmarty, C. J., C. Leveque, and C. Revenga (2005), Freshwater ecosystems, in *Millennium Ecosystem Assessment*, vol. 1, *Conditions and Trends*, edited by C. Caudill et al., chap. 7, pp. 165–207, Isl. Press, Washington, D. C.
- Wada, Y., L. P. H. van Beek, and M. F. P. Bierkens (2011a), Modelling global water stress of the recent past: On the relative importance of trends in water demand and climate variability, *Hydrol. Earth Syst. Sci.*, 15(12), 3785–3808.
- Wada, Y., L. P. H. van Beek, D. Viviroli, H. H. Durr, R. Weingartner, and M. F. P. Bierkens (2011b), Global monthly water stress: 2. Water demand and severity of water stress, *Water Resour. Res.*, 47, W07518, doi:10.1029/2010WR009792.
- Wada, Y., L. P. H. van Beek, N. Wanders, and M. F. P. Bierkens (2013), Human water consumption intensifies hydrological drought worldwide, *Environ. Res. Lett.*, 8(3), 034036.
- Wada, Y., T. Gleeson, and L. Esnault (2014a), Wedge approach to water stress, *Nat. Geosci.*, 7(9), 615–617.
- Wada, Y., D. Wisser, and M. F. P. Bierkens (2014b), Global modeling of withdrawal, allocation and consumptive use of surface water and groundwater resources, *Earth Syst. Dyn. Discuss.*, 5, 15–40.
- Wada, Y., I. E. M. de Graaf, and L. P. H. van Beek (2016), High-resolution modeling of human and climate impacts on global water resources, *J. Adv. Model. Earth Syst.*, 8, 735–763, doi:10.1002/2015MS000618.
- Wang, C., H. Wang, and A. Xarapat (2011), Spatial and temporal changes of lake wetlands in Jiangnan Plain after the implementing of 'thirty-six word policy', *Procedia Environ. Sci.*, 10, 2574–2580.
- Wang, J. (2013), *Lake dynamics in the Yangtze Basin downstream of Three Gorges Dam driven by natural determinants and human activities*, PhD dissertation, Dep. of Geogr., Univ. of Calif., Los Angeles.
- Wang, J., Y. Sheng, C. J. Gleason, and Y. Wada (2013), Downstream Yangtze River levels impacted by Three Gorges Dam, *Environ. Res. Lett.*, 8, 044012.
- Wang, J., Y. Sheng, and T. S. D. Tong (2014a), Monitoring decadal lake dynamics across the Yangtze Basin downstream of Three Gorges Dam, *Remote Sens. Environ.*, 152, 251–269.
- Wang, J., Y. Sheng, and T. S. D. Tong (2014b), Satellite-based daily lake areas in the Yangtze Basin, China, 2000–2011, *PANGAEA*, doi:10.1594/pangaea.841056.
- Wei, X., Y. Du, Z. Zhang, Z. Qiao, and F. Liu (2009), Study of historical changes of lake landscape in the middle reaches of the Yangtze, paper presented in 3rd International Conference on Bioinformatics and Biomedical Engineering, Inst. of Electr. and Electr. Eng., Beijing.
- Weiland, F. C. S., J. A. Vrugt, R. P. H. van Beek, A. H. Weerts, and M. F. P. Bierkens (2015), Significant uncertainty in global scale hydrological modeling from precipitation data errors, *J. Hydrol.*, 529, 1095–1115.
- Wint, W., and T. Robinson (2007), *Gridded livestock of the world 2007*, report, 131 pp., Food and Agric. Org. of the U. N., Rome, Italy.
- World Resources Institute (1998), *World Resources, 1998–99: A Guide to the Global Environment*, Oxford Univ. Press, New York.
- Wu, G. P., and Y. B. Liu (2015), Capturing variations in inundation with satellite remote sensing in a morphologically complex, large lake, *J. Hydrol.*, 523, 14–23.
- Xie, P. P., and P. A. Arkin (1997), Global precipitation: A 17-year monthly analysis based on gauge observations, satellite estimates, and numerical model outputs, *Bull. Am. Meteorol. Soc.*, 78(11), 2539–2558.
- Xu, K. H., and J. D. Milliman (2009), Seasonal variations of sediment discharge from the Yangtze River before and after impoundment of the Three Gorges Dam, *Geomorphology*, 104(3–4), 276–283.
- Yang, S., Q. Zhao, and I. Belkin (2002), Temporal variation in the sediment load of the Yangtze River and the influences of human activities, *J. Hydrol.*, 263, 56–71.
- Yang, S. L., J. Zhang, and X. J. Xu (2007), Influence of the Three Gorges Dam on downstream delivery of sediment and its environmental implications, Yangtze River, *Geophys. Res. Lett.*, 34, L10401, doi:10.1029/2007GL029472.
- Yang, S. L., J. D. Milliman, K. H. Xu, B. Deng, X. Y. Zhang, and X. X. Luo (2014), Downstream sedimentary and geomorphic impacts of the Three Gorges Dam on the Yangtze River, *Earth Sci. Rev.*, 138, 469–486.
- Yang, S. L., K. H. Xu, J. D. Milliman, H. F. Yang, and C. S. Wu (2015), Decline of Yangtze River water and sediment discharge: Impact from natural and anthropogenic changes, *Sci. Rep.*, 5, 12581, doi:10.1038/srep12581.
- Yang, X., and X. X. Lu (2013), Delineation of lakes and reservoirs in large river basins: An example of the Yangtze River Basin, China, *Geomorphology*, 190, 92–102.

- Yang, Z., H. Wang, Y. Saito, J. D. Milliman, K. Xu, S. Qiao, and G. Shi (2006), Dam impacts on the Changjiang (Yangtze) River sediment discharge to the sea: The past 55 years and after the Three Gorges Dam, *Water Resour. Res.*, *42*, W04407, doi:10.1029/2005WR003970.
- Ye, X., Q. Zhang, J. Liu, X. Li, and C.-y. Xu (2013), Distinguishing the relative impacts of climate change and human activities on variation of streamflow in the Poyang Lake catchment, China, *J. Hydrol.*, *494*, 83–95.
- Ye, X., Y. Li, X. Li, and Q. Zhang (2014), Factors influencing water level changes in China's largest freshwater lake, Poyang Lake, in the past 50 years, *Water Int.*, *39*(7), 983–999.
- Yésou, H., et al. (2011), Nine years of water resources monitoring over the middle reaches of the Yangtze River, with ENVISAT, MODIS, Beijing-1 time series, Altimetric data and field measurements, *Lakes Reservoirs Res. Manage.*, *16*, 227–243.
- Yuan, Y. J., et al. (2015), Variation of water level in Dongting Lake over a 50-year period: Implications for the impacts of anthropogenic and climatic factors, *J. Hydrol.*, *525*, 450–456.
- Zarfl, C., A. E. Lumsdon, J. Berlekamp, L. Tydecks, and K. Tockner (2015), A global boom in hydropower dam construction, *Aquat. Sci.*, *77*(1), 161–170.
- Zhang, Q., L. Li, Y. G. Wang, A. D. Werner, P. Xin, T. Jiang, and D. A. Barry (2012), Has the Three-Gorges Dam made the Poyang Lake wetlands wetter and drier?, *Geophys. Res. Lett.*, *39*, L20402, doi:10.1029/2012GL053431.
- Zhang, Q., X. Ye, A. D. Werner, Y. Li, J. Yao, X. Li, and C. Xu (2014), An investigation of enhanced recessions in Poyang Lake: Comparison of Yangtze River and local catchment impacts, *J. Hydrol.*, *517*, 425–434.
- Zhang, Z. X., X. Chen, C. Y. Xu, Y. Hong, J. Hardy, and Z. H. Sun (2015), Examining the influence of river-lake interaction on the drought and water resources in the Poyang Lake basin, *J. Hydrol.*, *522*, 510–521.
- Zhang, Z. Z., B. F. Chao, J. L. Chen, and C. R. Wilson (2015), Terrestrial water storage anomalies of Yangtze River Basin droughts observed by GRACE and connections with ENSO, *Global Planet. Change*, *126*, 35–45.
- Zhao, S. Q., and J. Y. Fang (2004), Impact of impoldering and lake restoration on land-cover changes in Dongting Lake area, Central Yangtze, *Ambio*, *33*(6), 311–315.
- Zhao, X., J. Liu, Q. Liu, M. R. Tillotson, D. Guan, and K. Hubacek (2015), Proceedings of the National Academy of Sciences, *112*(4), 1031–1035.
- Zhou, B., S. Xie, Y. Xiao, X. Liu, J. Liang, G. Zeng, and C. Du (2015), Changes of beach and genetic analysis in the Dongting Lake wetland during the initial running of the Three Gorges Project [in Chinese], *J. Water Resour. Res.*, *4*, 81–87.